CONTRIBITION OF DNA HELICASES TO GENOME STABILITY

Grzegorz Zapotoczny

A dissertation submitted to the faculty of the University of North Carolina at Chapel Hill
in partial fulfillment of the requirements for the degree of Doctor of Philosophy in the
Curriculum in Genetics and Molecular Biology.

Chapel Hill
2016

Approved by:

Jeff Sekelsky

Gregory Copenhaver

Robert Duronio

Thomas Petes

Dale Ramsden

ABSTRACT

Grzegorz Zapotoczny: Contribution of DNA helicases to genome stability
(Under the direction of Jeff Sekelsky)

DNA double-strand breaks (DSBs) are one of the most deleterious lesions to the cell.

Even a single unrepaired DSB can lead to apoptosis, recombination, loss of heterozygosity, and

cancer, thus it is essential for DSBs to be repaired. Synthesis-dependent strand annealing

(SDSA) is thought to be a major pathway of DSB repair in mitotically dividing cells, yielding

non-recombinant products. Assays that directly measure SDSA have been used to study SDSA in

fruit flies and yeast, however, in humans SDSA is poorly understood and the players involved

are unknown due to the lack of an SDSA assay. I have developed the first SDSA assay in human

cells and present the first direct evidence for SDSA in humans. Furthermore, I report here that

human BLM helicase, unlike its Drosophila ortholog is a negative regulator of SDSA. I

identified RTEL1 as another negative SDSA regulator. This study provides new insights into the

molecular basis of SDSA regulation and shows that BLM and RTEL1-deficient cells exhibit

longer synthesis tracts which facilitates SDSA repair. To complement my studies, I utilized a

DR-GFP assay to measure GC levels and engineered a crossover-gene conversion (CO-GC)

assay and demonstrate here that BLM is responsible for suppression of COs in human cells

despite its inhibitory effect on SDSA.

To all the people of good heart who made this chapter of my life special :)

ACKNOWLEDGEMENTS

I would like to thank my advisor, Jeff Sekelsky, for saving all the most challenging projects for me, but never leaving me all by myself with them. Thank you for fostering my independence, giving me lots of freedom, and supporting my research ideas.

Thank you to my committee for your constant support and expertise. I appreciate the effort you put in making me a better scientist, whether helping me see the bigger picture or with constructive criticism.

I would like to thank all my labmates for not only being mere coworkers but becoming true friends. Bonding over failed experiments or personal struggles made the Sekelsky lab feel like a family. Thank you to Stephanie for being my rotation mentor and a "bench wife", and Danielle for always rescuing me in crisis, like getting locked out of the tissue culture room in the middle of the night. Great thanks to Nicole and Lydia for improving my science writing skills and serving as role models. Thank you to Julie for always being prepared and willing to share, whether a bike pump, a canister of gas, or a simple toothpaste. Thank you to Susan for bringing Jonah to the lab and letting me play with him, and to Talia for her energy and contagious enthusiasm.

I would like to thank all my friends for being there for me despite I could not always be there for them working late nights in the lab. Great thanks to Jen for being my dance partner, Josh for talking science with me, Andrew for incorporating his industrial design talents into my work, and Luke for reading my papers and being the "grammar police".

Most importantly, I would like to thank my Polish family for always believing in me and supporting me remotely, my US family for letting me celebrate holidays with them, and my Chapel Hill church family for inviting me to be a part of their daily activities and letting me serve as a role model for their kids. I would not have made it without you.

CONTRIBUTIONS

TABLE OF CONTENTS

LIST OF FIGURES

LIST OF TABLES

LIST OF ABBREVIATIONS

bp – base pair

CO – crossover

dHJ – double Holliday junction

D-loop – displacement look

DSB – double-strand break

DSBR – double-strand break repair

FA – Fanconi anemia

GC – gene conversion

hDNA – heteroduplex DNA

HJ – Holliday junction

HR – homologous recombination

LOH – loss of heterozygosity

MMEJ – microhomology-mediated end joining

NCO – non-crossover

NHEJ – non-homologous end-joining

nt – nucleotide

SDSA – synthesis-dependent strand annealing

SSA – singe-strand annealing

TEMJ – Theta-mediated end-joining

TLS – trans-lesion synthesis

<center>**CHAPTER 1**</center>

<center>**INTRODUCTION**</center>

DNA and Genome Stability

DNA is the carrier of genetic information, and its integrity is essential for proper functioning of all cells. The DNA of all living organisms is prone to damage from both exogenous (UV and gamma radiation, chemicals) and endogenous (free radicals and reactive oxygen species, stalled or collapsed replication forks) sources. Among of the most dangerous to the cells are DNA damaging agents that cause double-strand breaks (DSBs). Even a single DSB can lead to cell apoptosis, loss of heterozygosity (LOH) of a tumor suppressor gene, and thus eventually to cancer. Therefore, understanding how DSBs are repaired and identifying the players involved in this process is of great priority.

Since the discovery of the DNA double-helix structure by Watson and Crick (Watson and Crick, 1953), there has been a tremendous progress in the field of DNA damage repair. Our continuous effort to further the knowledge of the very processes that keep us alive and their extreme importance has been reemphasized by awarding last year Noble Prize to three great scientists: Aziz Sancar, Tomas Lindhal, and Paul Modrich, for their contributions to the DNA damage repair field.

DNA Double strand break repair model

DNA double strand breaks (DSBs) can be repaired via either non-homologous end joining (NHEJ) or homology-directed repair (HR) (Symington, 2002). NHEJ is very efficient and

<center>1</center>

cost-effective but can often generate mutations. HR is thought to be a DSB repair pathway assuring fidelity during repair and a cell's primary choice after DNA replication is complete and a sister-chromatid is available as a template for the repair.

The HR model of double-strand break repair (DSBR), proposed by Jack Szostak, Terry Orr-Weaver, and Rodney Rothstein based on their research conducted in Frank Stahl's laboratory in yeast, has been found to be conserved in all diploid organisms studied thus far (**Fig. 1**) (Szostak et al., 1983).
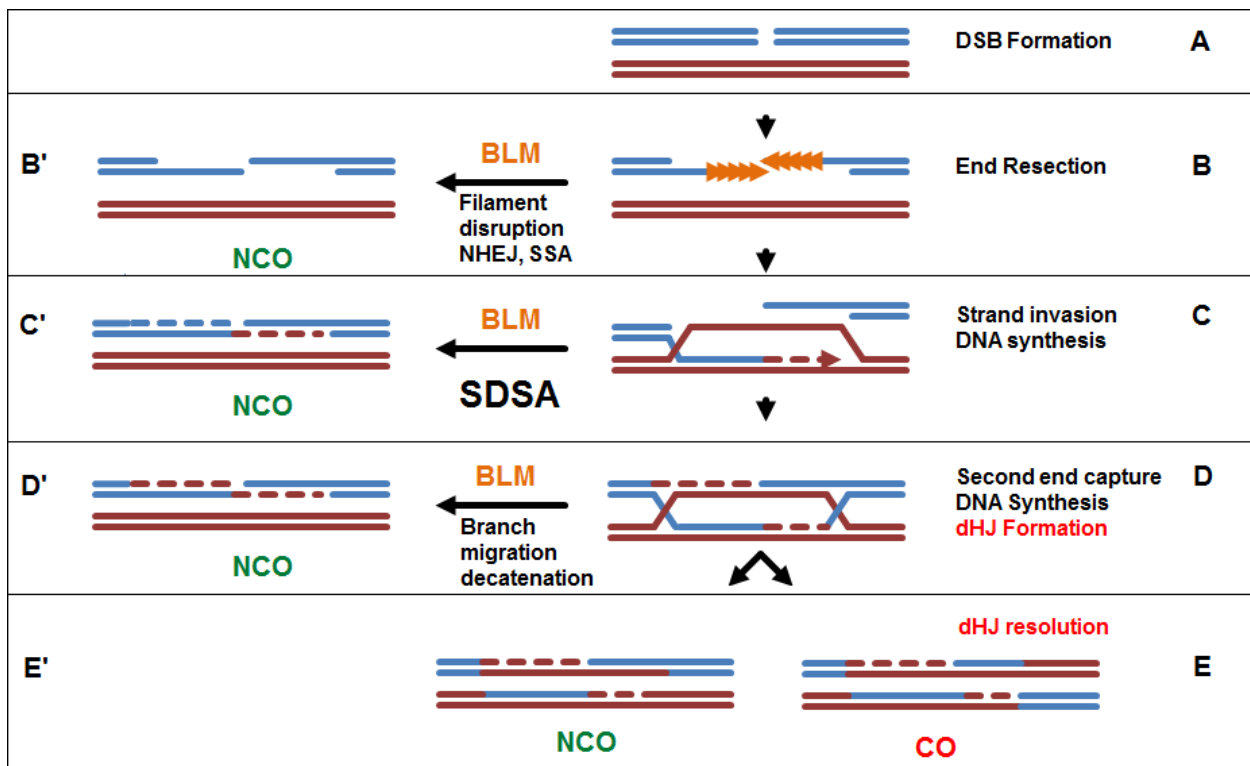
Figure 1. Model for the DNA DSBs via HR.
The canonical DSB repair model proposed by Szostak *et al* (Szostak et al 1983) predicts that the ends of DSB (A) are resected (B) to form 3' overhangs, which then invade homologous template to create a D-loop and prime synthesis (C). Subsequent DNA ligation leads to a dHJ intermediate formation (D), which then can be further processed into CO (E) or NCO (E') by HJ resolvases. DNA helicases such as BLM can act on different repair intermediates to promote NCO formation by supporting NHEJ or SSA (B') SDSA (C') or dHJ dissolution (D'). See text for details.

Upon DSB formation (**Fig. 1A**) HR orchestrates resection of the DNA 5' ends so that remaining 3' single-stranded ends **(Fig. 1B)** can invade the homologous chromosome or sister chromatid and use them as templates for synthesis creating a displacement loop (D-loop) (**Fig. 1C**). The homology search is one of the least known mechanisms of the DSBR, however, we know that Rad51, in humans loaded by BRCA2, is essential (**Fig. 1B** orange triangles). According to this most frequently cited model for HR, further processing generates an intermediate with two Holliday junctions (HJs; **Fig. 1D**). A HJ is a structure of two interconnected DNA helices that must be resolved for proper chromosome separation. The HJs are cleaved by specialized endonucleases, called resolvases, to generate either a crossover (CO; **Fig. 1E**) or non-crossover (NCO**; Fig. 1E'**). Either can be associated with gene conversions, in which the exchange of genetic material is unidirectional.

Although HR is considered to be error-free, there are potential hazards involved in its execution that must be avoided. In proliferating cells, in particular, COs (reciprocal or bidirectional exchanges of genetic material) between homologous chromosomes are not desired because they may lead to LOH (LaRocque et al., 2011; Wang et al., 2011)). LOH has been implicated in carcinogenesis as a major mechanism that leads to the loss of functional copies of tumor suppressor genes (Knudson, 1971; Luo et al., 2000). COs can also lead to chromosome rearrangements in cases of ectopic recombination between DNA duplications (Cong et al., 2013).

Knowing that DSBs are rarely repaired as crossovers in mitotically proliferating cells (Andersen and Sekelsky, 2010), a pathway of HR that results in mostly NCOs must be employed (**Fig. 1B'; 1C'; 1D'**). Previous work by us and others led to a model that proposes DSBs in mitotic cells are being repaired by SDSA (**Fig. 1C'**). The SDSA model predicts that DNA helicases, such as Bloom helicase (BLM), act to unwind recombination intermediates that lead to

COs, thus forcing the break to be repaired as a NCO (Andersen et al., 2011). Testing this model has proven to be very challenging before the development of proper tools, namely DSBR assays, which allow gaining insights into the repair outcomes and pathway choices in model organisms.

The history of DNA DSBR assays

Drosophila melanogaster **assays**

The first *Drosophila* DSBR assay was developed in the Engels laboratory in 1991 (Gloor et al., 1991). These fruit fly geneticists took advantage of the *D. melanogaster* genome containing DNA transposons, called P-elements, which are mobilized upon introduction of the source of an enzyme called transposase. Transposase cuts out the P-element leaving a gap which is essentially a form of a DSB. These type of assays are often referred to as "gap repair assays". The biggest advantage of this assays is its simplicity and ability to perform a molecular analysis of the repair events. They were able to look at 123 conversion tracts and map them using restriction digest and sequencing. Interestingly, even though the average tract length was 1379 base pair (bp), the longest ones were even a few thousands bases long. Their results indicated an existence of an unknown DSBR pathway with a "dissolution" of the recombination intermediate before second end capture. Although they never mentioned it, the characteristics of this pathway indicate it was likely SDSA.

A few years later, Engel's group coined the term SDSA and formulated a model that encompasses the experimental observations (Nassif et al., 1994). They were able to demonstrate nearly 8 kilo-bases (kb) long DNA synthesis tracts upon P-element excision that came not only from a sister chromatid, but also from a homologous but ectopic template. The patterns of repair indicated that each terminus of the break acted independently from one another to prime

synthesis, yielding two single-stranded overlapping sequences. The two ends would then anneal to one another and be further extended to fill in the entire gap.

It was not until 2003 when the first high throughput, SDSA-specific assay, called $P\{w^a\}$, adapted from Kurkulos and Mount (Kurkulos et al., 1994), was utilized in the Sekelsky laboratory (Adams et al., 2003). In this assay, the $P\{w^a\}$ transposon carries a copy of the *apricot* (w^a) allele of the *white* (*w*) gene, which carries an insertion of a 5-kb *copia* retrotransposon. The *copia* long terminal repeats (LTR) are about 5-kb from each *P* element end. During gap repair, annealing of both single-stranded DNA ends at the two LTRs results in loss of the *copia* element. This outcome, which is easily distinguished phenotypically from the starting $P\{w^a\}$ transposon by the change of the flies' eyes color, cannot be explained by the canonical DSBR model, so it is believed to uniquely identify SDSA repair. Another feature of this assay is the ability to analyze molecularly the events that failed to complete SDSA. The synthesis that does not reach LTRs yields a hypomorphic or amorphic alleles of *white* which is exhibited by the presence of yellow or white-eyed flies. The ratio between flies with different eye-colors is an excellent indicator of the SDSA repair success rate and allows utilizing a reverse genetics approach to determine the key players involved in this process. This state of the art SDSA assay was also used to demonstrate that the strand invasion and synthesis during SDSA is not a single, static event but rather consists of multiple evasions events capable to synthesize across a 14kb long gap (McVey et al., 2004a).

Saccharomyces cerevisiae assays

The first yeast gap repair assay came from the Haber laboratory and involved the repair of HO endonuclease-induced DSBs (Pâques et al., 1998). What makes it a gap repair assay is the

unique design of the repair template that consists of 375bp-long repeats placed in the middle of the sequence homologous to the DSB surrounding area. The greatest strength of the assay is the ability to provide different repair templates, whether on a donor plasmid or integrated into the genome. Interestingly, the repair efficiency was inversely correlated with the complexity of the template and the size of the gap, with genomic templates utilized more efficiently that the ectopic ones. However, the main observation from this study was the existence of incorrect or unfaithful copying of the repair template which was exhibited by either contractions or duplications of the tandem repeats. Whether by slippage accompanying the synthesis after the second-end capture and the dHJ formation, or by random pairing and annealing at the repeats during SDSA, it is unclear. This assay, however, provided strong evidence for the existence of an alternate to the Szostak's canonical DSBR pathway. Also, in yeast meiosis, upon tetrad and DNA heteroduplex analysis, some recombination events are not easily explained by the DSBR model, but rather exhibit features of the SDSA repair (Merker et al., 2003).

The first SDSA assay in yeast came from the Kusano laboratory (Miura et al., 2012) and is, in fact, capable of differentiating between both SDSA and NHEJ events. The assay is comprised of a plasmid carrying a *ura3* gene with an internal deletion and an *I-Sce*I recognition site where the DSB is generated, and two chromosomal templates for the repair that consist of either a 3' or the 5' *ura3* fragment. Functional *URA3* gene restoration is contingent upon synthesizing genetic information from both of the templates for the total of 458 nucleotides from which only 300 nucleotides is overlapping. Successful annealing at the 300-nt overlap is then scored as an SDSA event, while the restoration of an intact or disrupted *I-Sce*I sequence is recorded as an NHEJ event (precise or imprecise NHEJ respectively). This powerful system allows scoring hundreds of repair events and analyzing them molecularly. A putative weakness

of this assay, however, is using a plasmid that was not integrated to the genome, meaning it may not have been chromatinized. As shown in *Drosophila* cells, the chromatin context is extremely important; DSBR in heterochromatin is tightly regulated to promote HR and prevent NHEJ (Chiolo et al., 2011; Ryu et al., 2015).

Mammalian cell assays

In mammalian cells, direct-repeat GFP (DR-GFP) assay developed in the Jasin laboratory, is one of the most known and utilized tools for probing roles of various proteins in DSB repair (Pierce et al., 1999). Although originally designed for mouse cells, DR-GFP was adapted to various human cell lines like HEK293 or U2OS (Paliwal et al., 2014). In this assay, an upstream *GFP* gene (*SceGFP*) is disrupted by insertion of an *I-Sce*I site. A downstream *GFP* fragment (*iGFP*) serves as a template for repair. Gene conversion replaces the *I-Sce*I site with *GFP* sequences, generating an intact *GFP* gene. Gene conversion in this assay has been interpreted as arising through SDSA (Paliwal et al., 2014), but there are no features that distinguish between SDSA and DSBR.

Another gene conversion assay came from the Scully laboratory and although does not look specifically at SDSA, its unique feature is an ability to examine not only the levels of GCs, but also whether the synthesis tracts are long of short (Chandramouly et al., 2013). The design is similar to the DR-GFP assay, however should the 3' end extension continue past the *GFP* gene, and use a sister chromatid as a template, a distal end of *RFP* is copied and a red fluorescence is gained. This allows simultaneously screening for short-tract gene conversions (STGC) and long-tract gene conversions (LTGC).

Xu *et al.* developed a novel human cell assay in which gene conversion could be detected simultaneously at the DSB site and at another site about one kilobase pair (kb) away (Xu et al., 2012). They found that the two were often independent and concluded that SDSA is a major mechanism for DSB repair in human cells, but they could not exclude DSBR as a possible source.

Development of the CRISPR/Cas9 system for genome engineering (Cong et al., 2013; Mali et al., 2013) opened up new possibilities in terms of introducing DSBs and creating DSBR assays. It is suggested, replacement of multi-kilobase fragments after Cas9 cleavage most likely occurs through SDSA (Byrne et al., 2015), but this has not been directly tested. Although it is speculated, there is no direct evidence confirming SDSA existence in human cells, as no human SDSA assays have been developed just yet.

Features of an ideal DSBR assay

Just as DSBR is essential for genome stability and proper maintenance, clarity of DSBR assays is essential for their proper interpretation. One of the biggest issues of the human assays utilized to study DSBR outcomes to date is their ambiguity in determining the exact DSB's fate.

An ideal DSBR assay would be capable of differentiating between SDSA and other HR repair outcomes such as COs or GCs associated with dHJ resolution or dissolution. Another important feature is the ability to analyze repair events on a molecular level either by sequencing or PCR-based methods. Whole organism assays provide more physiological conditions, however, cell-based assays allow for higher reproducibility and an analysis of hundreds of thousands events, if not millions. Standardized and automatized systems, especially if they

utilize a presence of fluorescent markers and flow cytometry, will surpass the naked eye and subjectivity during data collection.

With an increasing understanding of epigenetics, the importance of DNA and histone modifications, in determining the DNA's accessibility to repair machinery, it is evident chromosomal assays provide more accurate insights into repair mechanisms than the plasmid-based ones. Multiple repair templates, especially if containing single-nucleotide polymorphisms (SNPs) to identify the source of the DNA sequence, provide more mechanistic details than other assays that cannot determine whether one or both DSB ends are involved in the homology search and priming DNA synthesis. Last but not least, DSB itself and how it is generated is of great importance. P-element excision rate is low but engineering a repair template is not needed as the intact sister-chromatid is always available in post-replication cells. Adenoviral-delivered I-SceI, which has an 18nt long recognition sequence normally absent in the human genome, is not only very specific but also effective with up to 85% cutting efficiency as measured in HEK293 cells (Anglana and Bacchetti, 1999). High cutting efficiently for endonucleases is vital as uncut *I-Sce*I and the product of precise NHEJ are indistinguishable. Processing of the Cas9-generated DSBs is still poorly understood, but it is conceivable to think DNA blunt ends created this way might undergo a different type of processing than DSBs composed of 3' or 5' overhangs.

All of these features are crucial for accurate data interpretation, especially when trying to compare the results in the backgrounds deficient or devoid of DSBR candidate proteins. DNA helicases, for instance, have been implicated in many processes pertaining to DNA repair and replication but their exactly role in human cells has been elusive due to the lack of precise assays to study them.

DNA helicases involved in DSBR repair

DNA helicases is a group of evolutionarily conserved enzymes utilizing energy from ATP hydrolysis to traverse across a double-stranded DNA molecule breaking hydrogen bonds between nucleotides in the process. Helicases recognize specific DNA structures, like HJs or D-loops, and bind single-stranded DNA. Depending on the type, helicases can travel either in the 3'→5' or 5'→3' direction to migrate or disassemble recognized DNA structures (van Brabant et al., 2000; Wu and Hickson, 2006). The vast majority of helicases belong to two superfamilies, SF1 and SF2. Their classification into families is based on the sequence of the helicase domain core (Fairman-Williams, 2010). DNA helicases implicated in DNA damage repair (**Table 1**) are members of a few families and the most of the mechanistic data about them derive from yeast. There are ongoing efforts to characterize human, and other model organisms' orthologs.

SF1: UvrD/ Rep family

S. cerevisiae Srs2 and human FBH1 are the two most studied members of this family. Srs2 is a 3'→5' helicase (Rong and Klein, 1993) and is structurally related to bacterial UvrD (Veaute, 2005). Copious evidence points out anti-crossover properties of Srs2 (Dervins, 2006; Ira et al., 2003) and its ability to negatively regulate HR via Rad51 nucleofilament disruption (Krejci, 2003; Veaute et al., 2003). Srs2 mutants exhibit a hyper-recombination phenotype (Rong, 1991), and a four-fold decrease in SDSA levels (Miura et al., 2012). Furthermore, Srs2 is important in avoiding LOH by promoting NCOs during HR (Miura, 2013).

Human FBH1 is also a 3'→5' helicase, however it is especially unique as it possesses an F-box motif that confers ubiquitin ligase activity (Kim, 2004). One of the FBH1 targets is Rad51 (Chu, 2015). FBH1 promotes an assembly of polyubiquitin chains on RAD51 that lead to its

inactivation which is thought to prevent unscheduled recombination at stalled DNA replication forks (Chu et al., 2015). Interestingly, expressing hFBH1 in *srs2* mutants rescues their viability in response to DNA damage, making hFBH1 a mammalian functional analog of Srs2 (Chiolo et al., 2007).

SF2: Rad3 family

RTEL1 is one of a few members of Rad3 family and its role in DSBR is largely unknown, likely because RTEL1 mutations are embryonic lethal in mice (Ding, 2004) and fruit flies (Morris et al, unpublished data). RTEL1-deficient ES cells exhibit decreased telomere length and proliferative capacity (Ding, 2004). Depletion of *RTEL1* in HeLa cells causes four-fold increase in the frequency of HR. Additionally, the cells become sensitive to mitomycin C, but not to IR (Barber et al., 2008). Although RTEL1 was initially identified as a telomere length regulator and is responsible for T-loop disruption (Sarek et al., 2015), biochemical studies indicate RTEL1can facilitate D-loop disassembly *in vitro* (Youds et al., 2010), thus could be an SDSA regulator. Furthermore, patients suffering from Dyskeratosis Congenita have been found to harbor *RTEL1* mutations (Savage and Alter, 2009).

SF2: RecQ family

There is only one RecQ helicase in yeast, Sgs1, but five in humans: BLM, WRN, RECQL1, RECQL4, and RECQL5. Mutations in *BLM*, *WRN*, and *RECQL4* are responsible for Bloom (Ellis et al., 1995), Werner (Yu et al., 1996), and Rothmund-Thomson (Kitato, 1999) syndromes respectively. Cells derived from the Bloom Syndrome patients exhibit high-levels of sister chromatid exchanges (SCE), which is a hallmark of recombination (Chaganti et al., 1974;

Wechsler et al., 2011). WRN and RECQL4 deficiencies do not cause SCE phenotype, but RECQL5 knockdown in mouse cells does; intriguingly, it has an additive effect when combined with siBLM treatment (Hu et al., 2005). Despite the similarity between BLM and RECQL5 in terms of SCE elevation phenotype, when these two helicases are knocked down in HEK293 and U2OS cells containing a DRGPF assay construct, siRECQ5 decreases GC levels while the siBLM unexpectedly increases GCs (Paliwal et al., 2014).

BLM helicase has multiple interacting partners and can act at various steps during HR. Exo-1, which is a 5'→3' dsDNA exonuclease, has been found to interact with BLM to resect DNA and initiate DSBR (Nimonkar et al., 2008). From all human RecQ helicases tested, only BLM was found to stimulate Exo-1resection activity, which would make BLM helicase a pro-recombination protein. At the same time BLM, and its yeast homolog Sgs1, can disrupt D-loops *in vitro* (Bachrati et al., 2006), promote SDSA in *D. melanogaster* (Adams et al., 2003; McVey et al., 2004a) and, in a complex with Topoisomerase 3 alpha, RMI1, and RMI2, catalyze dHJ dissolution (Singh et al., 2008; Wu and Hickson, 2003, 2006), emphasizing BLM's anti-crossover roles.

SGS1 was identified in a genetic screen for the suppressors of the *top3* slow growth phenotype (Gangloff et al., 1994). The *sgs1* phenotypes include slow growth, hyper recombination, and chromosome missegregation (Watt et al., 1996; Watt et al., 1995). Additionally, Sgs1 is required for non-crossover recombination in budding yeast meiosis (De Muyt et al., 2012).

SF2: Rig1-like family

Fanconi Anemia (FA) is a disorder caused by mutations in one of thirteen FA proteins which include FANCM helicase (yeast Mph1), but also BRCA1 and BRCA2 proteins. FA patients which exhibit high levels of chromosome instability, are susceptible to cancer, hypersensitive to interstrand-crosslinking agents such as mitomycin C (anti-cancer treatment drug), and have an increased chance of bone marrow failure (D'Andrea and Grompe, 2003; Huang et al., 2010; Meetei et al., 2005; Moldovan, 2009; Wang, 2007). The Drosophila FANCM just like BLM is found to promote SDSA (Kuo et al., 2014) and can disrupt D-loops in vitro (Romero et al., 2016). The *Arabidopsis* FANCM and RECQ4 have been found to promote non-crossover recombination during meiosis, possibly via SDSA (Crismani et al., 2012; Seguela-Arnaud et al., 2015). Likewise, in *Schizosaccharomyces pombe* during meiosis, Fml1, the ortholog of FANCM/Mhp1, was suggested to promote SDSA (Lorenz et al., 2012; Sun et al., 2008). Furthermore, the heteroduplex DNA analysis in yeast, that allows to differentiate between NCOs coming from SDSA or dHJ resolution, indicates that all three major yeast helicases, Sgs1, Srs2, and Mph1, are involved in promoting SDSA (Mitchel et al., 2013). The function of human orthologs of the aforementioned helicases in SDSA still remains to be elucidated.

Table 1. Helicase families and their selected members across species.

Family	RecQ	Rig1-like	UvrD/ Rep	Rad3
H. sapiens	BLM, WRN, RECQ5	FANCM	FBH1	RTEL1
D. melanogaster	BLM, RECQ5	FANCM	-	RTEL
S. cerevisiae	Sgs1	Mph1	Srs2	Rad3
A. taliana	RECQ4A, RECQ4B	FANCM	AtSRS2	RTEL1
E. coli	RecQ	-	UvrD	DinG

Scope of this work

      I conducted the work described in this dissertation to develop new tools to study DNA double-strand break repair in human cells, and investigate the role of DNA helicases in maintaining genome stability. First, I constructed and stably integrated an SDSA assay into human U2OS and HeLa cells. When I established that human cells utilize SDSA to repair DSBs, I used an siRNA approach to test various helicases for their SDSA regulation ability. I showed that BLM and RTEL1 are negative SDSA regulators, and performed a molecular analysis of the repair events when either of these helicases were depleted (Chapter 2). Furthermore, I used the DR-GFP assay developed in the Jason laboratory to find helicases involved in GC regulation (Chapter 3), and based on its design, I created another assay to look at the crossovers and gene conversions levels in human cells. Using the CO-GC assay, I was able to show that human BLM and FANCM helicases act to downregulate COs in mitotically diving cells (Chapter 3). Finally, I discuss all the results, propose a model for the roles BLM and RTEL1 in DSBR, present future experimental ideas, and outline suggestions to further improve our assays (Chapter 4).

CHAPTER 2

SYNTHESIS-DEPENDENT STRAND ANNEALING IN HUMAN CELLS

Introduction

Exactly 40 years ago, Michael Resnick proposed a theoretical model of the DNA double-strand break repair (DSBR) that involved a heteroduplex DNA (hDNA) intermediate leading to a non-reciprocal recombination (in other words: gene conversion-GC or non-crossover-NCO) (Resnick, 1976). In theory, after the initial 5'→3' resection of the double-strand break (DSB) ends, the remaining 3' end can invade a homologous chromosome and initiate synthesis, only to be soon unwound and reannealed to the other side of the DSB. It took nearly 20 years to prove, and name, this purely speculative model demonstrating DSBR, was indeed utilized by eukaryotic cells (Gloor et al., 1991; Nassif et al., 1994). Today, we know this model as synthesis-dependent strand annealing (SDSA) which is thought as a predominant pathway of DSBR in mitotically dividing cells preventing chromosomal rearrangements, loss of heterozygosity (LOH), and cancer (Bignon, 2004).

One of the greatest challenges of studying SDSA is that how the final product, a gene conversion (GC) or non-crossover (NCO), is indistinguishable from the final product of three other DSBR processes. Single-strand annealing (SSA), or synthesis-independent strand annealing, is thought to occur when a DSB is generated between two repeated sequences with long enough homology to facilitate annealing (Paliwal et al., 2014; Wang et al., 2011). SSA generates NCOs, but the byproduct of SSA is a deletion encompassing the sequence between the

15

two repeats. There are assays designed specifically to study SSA which contain a selectable

marker placed within the to-be-deleted sequence (Paliwal et al., 2014; Wang et al., 2011).

Szostak's model for DSBR predicts that a dHJ can be resolved into CO and NCO products

(Szostak et al., 1983). NCOs also arise from dHJ dissolution as a product of BTR complex

(BLM, Topoisomerase 3 alpha, RMI1, and RMI2) (Singh et al., 2008; Wu and Hickson, 2003,

2006). hDNA analysis can differentiate between NCOs coming from a dHJ intermediate (dHJ

dissolution and resolution), and those coming from a D-loop disruption (SDSA). dHJ dissolution

yields NCOs with hDNA on both sides of the gap, while dHJ resolution - in both cleavage

products, but SDSA yields hDNA only on one side of the gap (Mitchel et al., 2013).

Furthermore, Allers and Lichten demonstrated, at least during yeast meiosis, there is a

differential timing and control of NCO and CO recombination (Allers and Lichten, 2001). COs

and NCO that come from a dHJ intermediate appear later than NCOs coming from an

intermediate preceding dHJ (presumably via SDSA).

To date, there are only two SDSA assays, one in *Drosophila* named $P\{w^a\}$ (Adams et al.,

2003), the other in *S. cerevisiae* (Miura et al., 2012). Both of the assays present unique, but

different solutions to the SDSA identification dilemma. In the *Drosophila* SDSA assay, excising

the *copia* P-element within a *white* gene (hypomorphic apricot allele) creates a gap that can be

repaired either via SDSA or HR with a dHJ as an intermediate; SSA is not an option as there are

no repeated sequences in the vicinity of the break. The repair template is an intact sister

chromatid and thus, both dHJ dissolution and resolution yield products that are indistinguishable

from the initial sequence hence the flies maintain their apricot eye color phenotype. SDSA and

SDSA alone can facilitate annealing at the *copia* long terminal repeat (LTR) sequence within the

white gene resulting in the restoration of the wild type *white* gene; the flies exhibit a red eye

color phenotype. DSBR via end-joining in this assay results in a loss of a functional *white* gene hence the flies exhibit a white eye color phenotype. In the yeast SDSA assay, the I-SceI-generated DSB in a nonfunctional plasmid DNA *ura3* gene, cannot be repaired via dHJ-mediated pathways as the templates for the repair reside on two different chromosomes and the recombination between them would lead to lethal chromosomal rearrangements. SDSA and NHEJ are the only repair products retrievable in this assay, and only SDSA leads to the restoration of the functional *URA3* gene/5-FOA sensitivity.

Results

Human U2OS cells repair DSBs via SDSA

SDSA is thought to be a major pathway preventing COs and leading to NCO products. However, there is no direct evidence indicating that human cells utilize SDSA to repair DSBs. To assess the existence of SDSA in humans, I developed the first human SDSA assay (**Fig. 2**). The SDSA assay has an *mCherry* gene in which a 350-bp segment was replaced with the 18 bp *I-Sce*I recognition sequence, rendering the gene non-functional (**Fig. 2A**). Expression of *I-Sce*I enzyme generates a DSB (**Fig. 2B**). A split template for repair by HR is located downstream. Each half has 800 bp of homology adjacent to the break site plus the 350 bp of deleted *mCherry* sequence; these are separated by a 3-kb spacer of unique sequence (**Fig. 2A**). Since the 350-bp sequence is on both sides of the spacer, it constitutes a direct repeat similar to the *copia* LTRs of P{*w^a*}. Each end of the *I-Sce*I-induced break can invade the half of the template to which it is homologous, either simultaneously or sequentially (**Fig. 2C**). If synthesis on each side extends past the 350 bp repeat before the nascent strands are dissociated from the template, these regions can anneal to one another (**Fig. 2D**).
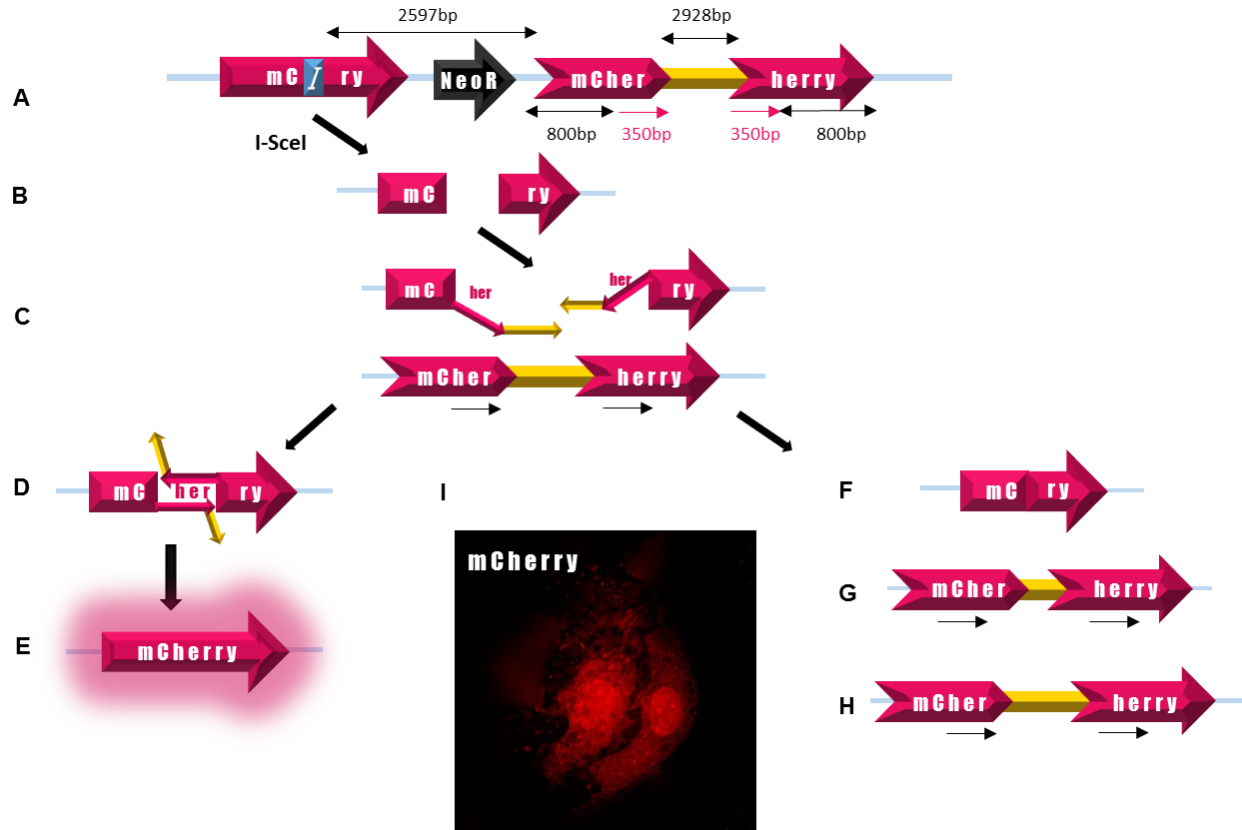
Figure 2. Human U2OS cancer cells undergo DSBR via SDSA.
(A) Human SDSA assay construct consisting of two *mCherry* halves (pink) interrupted but either I-SceI recognition sequence (White letter "I" on a blue background replacing 350bp sequence of the *mCherry* gene), or a Copia element (yellow); **(B)** I-SceI endonuclease recognizes a specific sequence and cuts the DNA creating a DSB; **(C)** 3' ends of the processed DSB invade the repair template priming synthesis; **(D)** disrupted synthesis that amplified 350nt long *mCherry* repeat leads to the annealing of the extended 3' ends; **(E)** a functional *mCherry* gene is restored and the cells that underwent SDSA repair are visible under the confocal microscope (Olympus FV1200; 60x objective) **(I)**; **(F)** NHEJ can repair DSB by ligating the two ends of the break together yielding a non-functional *mCherry* gene; **(G)** Disrupted SDSA followed by end-joining can lead to a partial synthesis and incorporation of the Copia element into the upstream *mCherry* yielding a non-functional *mCherry* gene; **(H)** Long and uninterrupted SDSA can lead to copying of the homologous template in place of I-SceI sequence yielding a non-functional *mCherry* gene.

Completion of SDSA (removal of any sequences extending into the spacer, filling in of gaps, and ligation) restores a functional *mCherry* gene at the upstream location (**Fig. 2E**). Sequential one-ended SDSA is also possible. If one end of the break invades the downstream template, is extended by repair synthesis, and then is dissociated from the template, the nascent strand will not be complementary to the other resected end; however, this nascent strand will be able to

engage with the other half of the repair template based on the 350-bp repeat to initiate a second cycle of strand exchange and repair synthesis, leading to the addition of sequences complementary to the other resected DSB end. This would also restore a functional *mCherry* gene by SDSA. A functional *mCherry* gene might also be generated through a combination of SDSA and DSBR. In the sequential SDSA scenario described above, the second strand exchange event could be processed into a dHJ. The product of dissolution or non-crossover resolution of such a dHJ will be identical to that of SDSA; however, if the dHJ is resolved as a crossover, generation of a functional *mCherry* gene it will be accompanied by a deletion of all sequences between the upstream *mCherry* and the downstream template. Dissolution or non-crossover dHJ resolution in this scenario cannot be distinguished from SDSA, but formation of such a dHJ intermediate does require at least one cycle of D-loop disassembly, a key step that distinguishes SDSA from DSBR.

Other types of repair that do not generate a functional *mCherry* are also possible (**Fig. 2F-H**). A dHJ can be generated if synthesis extends through one *mCherry* 350-bp repeat, the entire spacer, and the other 350-bp repeat. Processing of this dHJ would give a product in which the entire template, including the duplicated 350-bp sequences and the spacer, was copied into the upstream *mCherry* gene (**Fig 2H**). Dissolution or non-crossover resolution would result in two copies of the template, whereas crossover resolution would delete intervening sequences (**Fig. 2A** *neoR*). Non-homologous end joining (NHEJ) can restore or disrupt the *I-Sce*I recognition sequence, depending on whether it is precise or imprecise (**Fig. 2F**). Hybrid repair, in which repair is initiated by HR but completed by end joining instead of annealing, can give rise to an *mCherry* in which the 350-bp gap is not completely filled or, if synthesis extends into the spacer, with part of the spacer is copied into the upstream *mCherry* gene (**Fig. 2G**). SSA repair

would lead to a deletion of the sequence between the I-SceI and the proximal *mCherry* repeat, but will not lead to the restoration of the functional *mCherry* gene. SSA between the upstream *mCherry* and the distal *mCherry* repeat is impossible as there is no sequence overlap between these two DNA sequences.

To generate cell lines with the SDSA assay construct, I transfected U2OS cells with linearized pSDSA vector and used neomycin to select stably-integrated lines. To induce DSBs, I infected cells with an adenovirus expressing *I-Sce*I (Anglana and Bacchetti, 1999). I detected mCherry activity by fluorescence microscopy (**Fig. 2I**) as early as two days after viral infection. Stable expression persisted through months of cell culturing. Initial molecular analysis of genomic DNA from clones derived from single mCherry-positive cells confirmed the absence of the *I-Sce*I, restoration of a complete *mCherry* gene (**Fig. 3A**). In contrast, the molecular analysis of genomic DNA from mCherry-negative clones confirmed the presence of the *I-Sce*I, by both PCR and restriction digest (**Fig. 3B**).
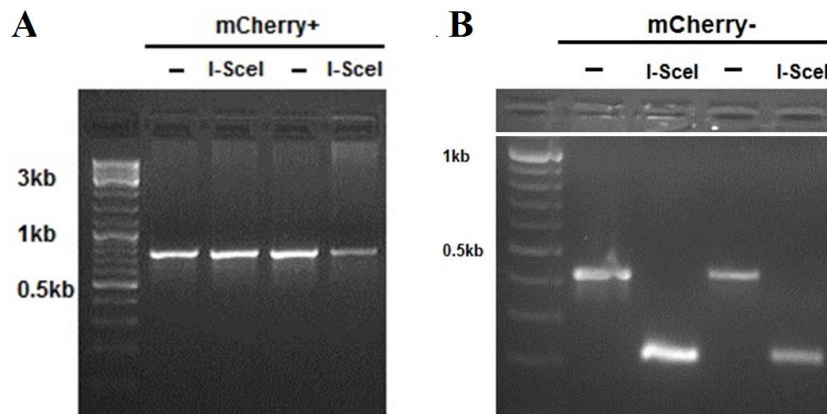
Figure 3. mCherry-positive clones are resistant to *I-Sce*I cutting while the mCherry-negative clones are susceptible.
Two images of 1.5% agarose gels with a PCR product using nhei_F and hindiii_R primers (see **Materials and Methods**). (**A**) Two different mCherry-positive clones were tested using a PCR for the presence of functional mCherry gene fluorescence (expected PCR product size: 783bp). As indicated, the clones were I-SceI resistant. (**B**) Two different mCherry-negative clones were tested using a PCR for the absence of the 350bp mCherry sequence that restores mCherry fluorescence (expected PCR product size: 433bp. As indicated, the clones were *I-Sce*I sensitive.

BLM and RTEL1 helicases are negative regulators of SDSA

The SDSA assay design allows high throughput data analysis using flow cytometry based on the cell size and fluorescence. Because U2OS cells adhere to the surface of the well, obtaining a single-cell suspension using trypsin-EDTA prior to analysis is necessary (see materials and methods). During harvesting a number of cell dies or is still attached to their neighbors despite the treatment. Gating strategy (**Fig. 4**) facilitates cell debris and doublet discrimination to score single mCherry-positive cells exclusively.
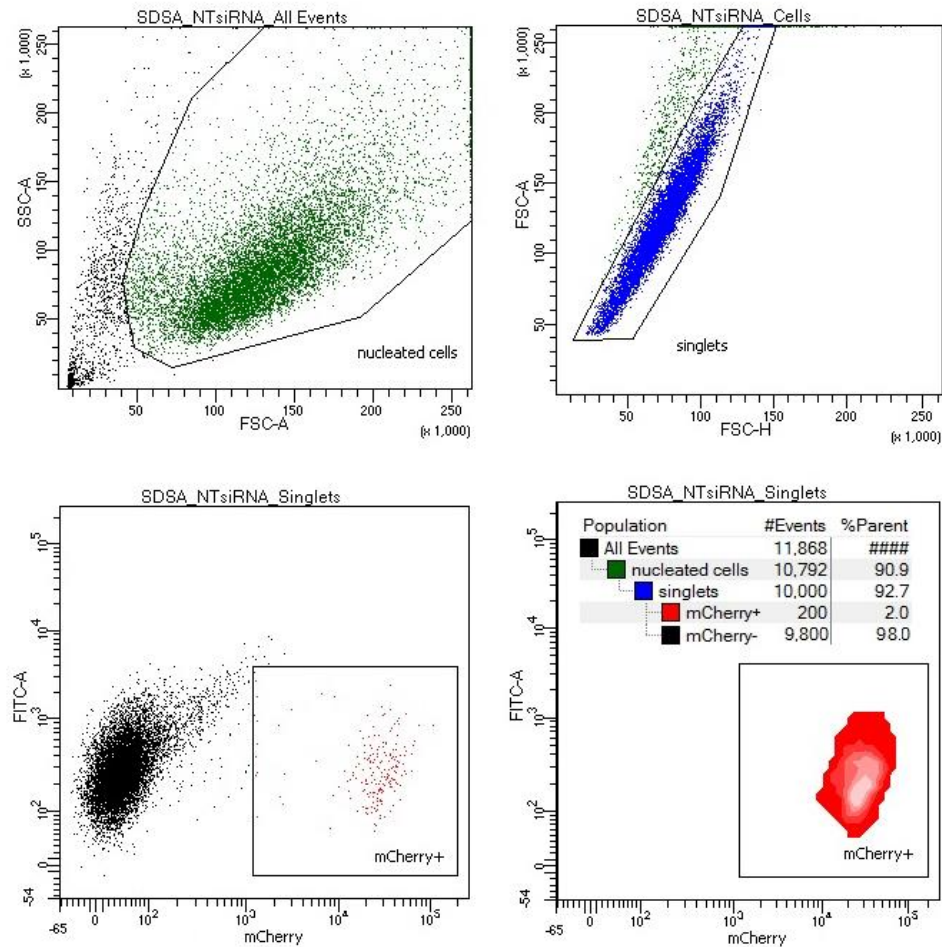
Figure 4. Flow cytometry facilitates analysis of SDSA events by detecting mCherry-positive cells. A representative siNT scatter plot shown. Forward and side scatter plots (FSC and SSC) allow identifying nucleated and single cells in a cell suspension (**top panels**). Cherry-positive cells are identified in the mCherry channel upon exposure to a yellow laser (**bottom panels**). Population hierarchy with accompanying statistics facilitates data recording and interpretation (**bottom right**)

BRCA2 is essential for RAD51-mediated strand exchange and thus SDSA (Sharan et al., 1997). To validate the SDSA assay, I knocked down BRCA2 in the SDSA-U2OS cells which yielded 50% reduction in SDSA (**Fig. 5A**). Residual SDSA in this experiment may have resulted from incomplete loss BRCA2 (**Fig 5B**)
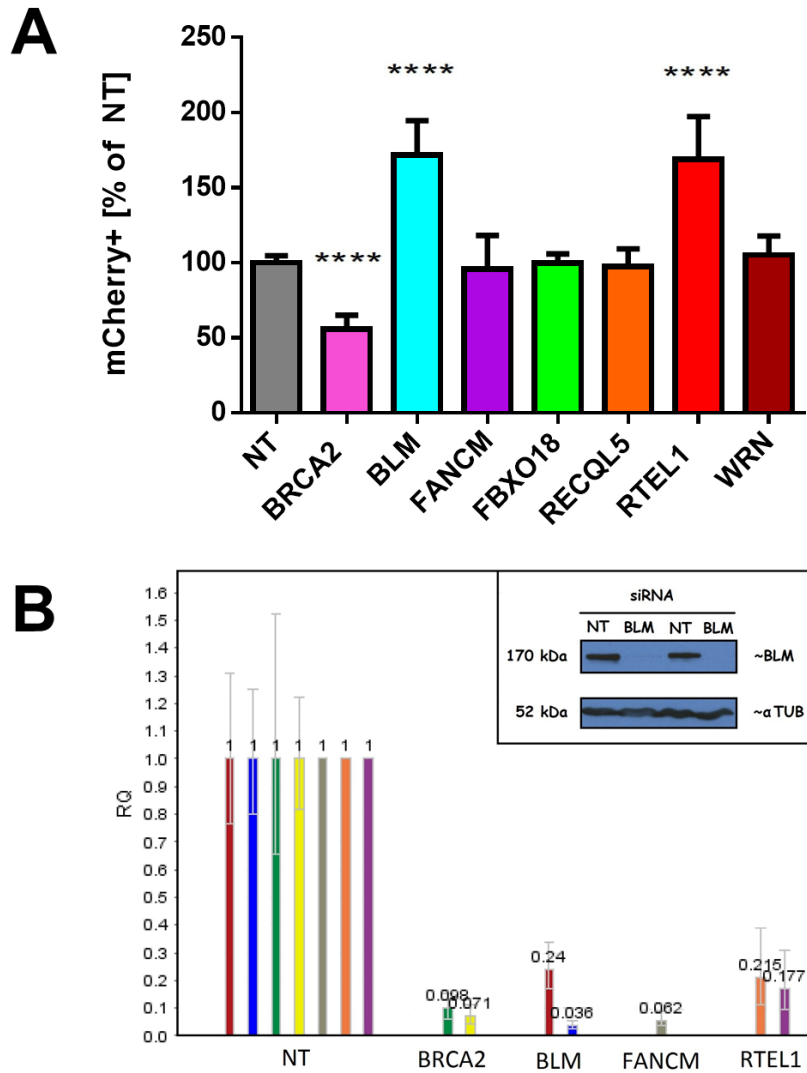
Figure 5. BLM and RTEL1 are negative regulators of SDSA in human cells.
(**A**) Relative SDSA frequency in SDSA-U2OS cells upon siRNA treatment. X-axis: different siRNA treatments; Y-axis: percent of the cells exhibiting mCherry fluorescence; values: averaged results of 12 experiments with 41 data points (NT); averaged results of 9 experiments with 31 data points (BLM); averaged results of 5 experiments with 20 data points (RTEL1); averaged results of 3 experiments with 7 data points (FANCM and RECQL5); averaged results of 2 experiments with 6 data points (FBXO18 and WRN) error bars: standard deviation; **** $p < 0.0001$
(**B**) qPCR analysis of the knockdown efficiency of BLM, BRCA2, FANCM, and RTEL1 and Western blot analysis of a BLM knockdown efficiency.

To determine which DNA helicases are involved in SDSA we used a candidate approach and selected a panel of genes consisting of: BLM, FANCM, FBXO18, RECQL5, RTEL1, and WRN for siRNA knockdown (see materials and methods). These helicases have been either previously implicated in DNA DSBR via HR in human cells or identified as positive SDSA regulators in model organisms (see introduction).

Surprisingly, BLM and RTEL1 helicase knockdowns resulted in a nearly two fold increase in the SDSA repair as measured by the percentage increase of the number of mCherry-positive cells standardized to a non-targeting siRNA control (**Fig. 5A**). Knocking down FANCM, FBXO18, RECQL5, or WRN did not result in a significant change in SDSA.

BLM and RTEL1 are BRCA2-dependent SDSA regulators

Both BLM and RTEL1 have multiple roles in genome maintenance. BLM, together with Dna2, can catalyze extensive DSB end resection, though this function is redundant with Exo1 (Zhu et al., 2008). BLM with Topoisomerase 3 alpha, RMI1, and RMI2 can catalyze dHJ dissolution (Singh et al., 2008; Wu and Hickson, 2003, 2006). RTEL1 was initially identified as a telomere length regulator and is responsible for T-loop disruption (Sarek et al., 2015). Biochemical studies indicate that RTEL1is responsible for D-loop disassembly, (Youds et al., 2010), but can unwind DNA secondary structures and promote replication fork progression (Vannier, 2013; Vannier and Sarek, 2014)

To assess whether BLM and RTEL1 act upstream or downstream from the homology search step during DSBR to regulate SDSA, I knocked down these helicases in combination with BRCA2, which is essential for homology search (Sharan et al., 1997). Consistent with this function, we observed a significant decrease in SDSA frequency when BRCA2 was knocked

down (**Fig. 5A and 6A**). When BRCA2 was knocked down simultaneously with BLM or

RTEL1, decreases of similar magnitude (relative to the increased SDSA frequency of BLM and

RTEL1 single knockdowns) were observed. I conclude that BLM and RTEL1 impact SDSA

through functions downstream of strand exchange into a homologous template.
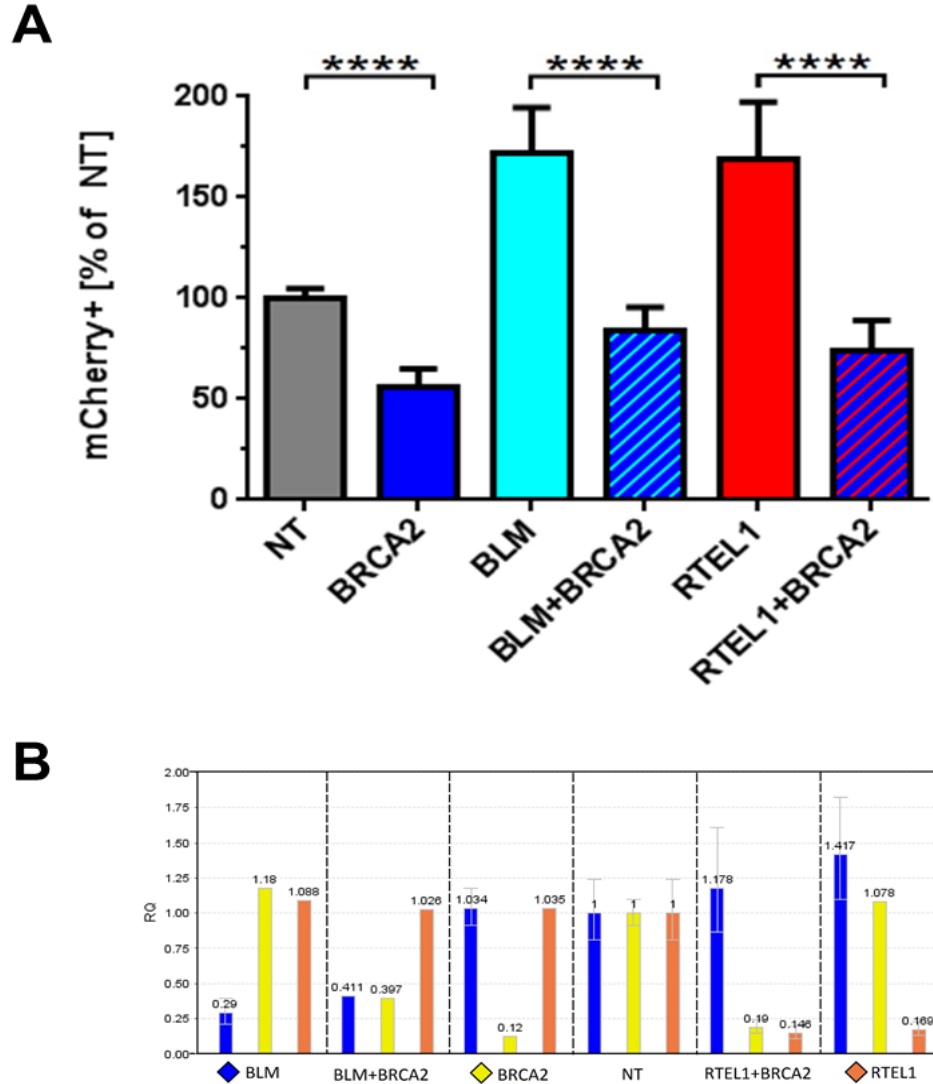
Figure 6. BLM and RTEL1 regulate SDSA in a BRCA2-dependent manner.
(A) Relative SDSA frequency in SDSA-U2OS cells upon siRNA treatment. X-axis: different siRNA treatments; Y-axis: percent of the cells exhibiting mCherry fluorescence; values: averaged results of 5 experiments (4 for double KDs) with 20 data points per treatment (16 data points per treatment for double KDs); error bars: standard deviation;
(B) qPCR of the knockdown efficiency of BLM, BRCA2, and RTEL1 from one representative experiment.

Knocking down BLM or RTEL1 results in different repair outcomes

To further develop our SDSA assay and gain additional insights into the effects of knocking down BLM and RTEL, I determined the structures of repair events produced in knockdown cells (**Fig. 7**). I analyzed 55 clones derived from single red-fluorescing cells, including 23 from the NT control, 21 from BLM knockdown, ten from FANCM knockdown, and one from RTEL1 knockdown. All but one had the structure expected of SDSA (**Fig. 2E**). The remaining clone, which came from non-targeting (NT) siRNA treatment, had lost *neo*^{R} and the template spacer, and therefore may have arisen from SDSA followed by DSBR with crossover resolution. These results support our conclusion that cells with restored *mCherry* utilized SDSA to repair the DSB, occasionally coupled with use of DSBR.
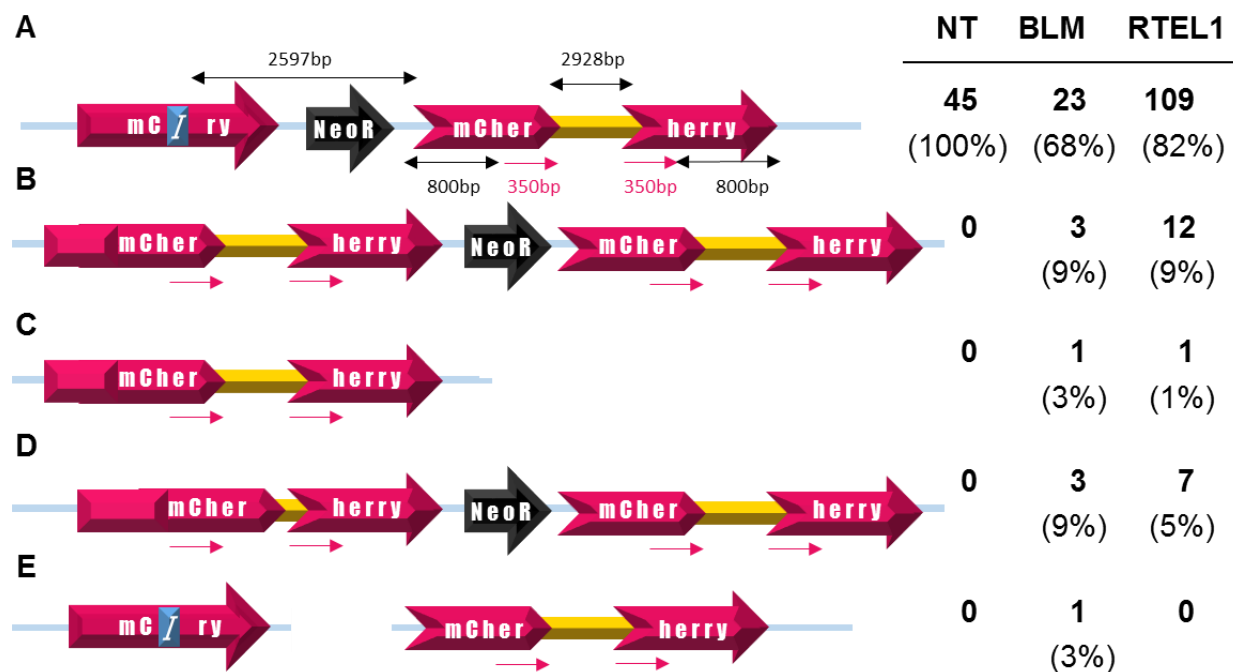
Figure 7. Structures of repair events in cells not expressing mCherry.
Single cells not expression red fluorescence were grown and then analyzed. (**A**) The starting construct, and the structure found in the majority of clones in each siRNA treatment group. (**B**) Copying of the entire template into the upstream *mCherry I-Sce*I site. (**C**) Copying of the entire template with loss of intervening sequences. (**D**) Copying of part of the template into the upstream *mCherry* site. (**E**) Retention of the *I-Sce*I site with loss of the *neo* and *ori* sequences.

I also analyzed cells that failed to produce mCherry to determine whether some of these were produced by other repair processes. In the non-targeting control, all 45 lines examined appeared to be identical to the initial construct (**Fig. 7A**). I titrated the viral concentration to a sublethal dose to obtain a maximal possible transfection efficiency, thus these events are likely the result of a precise NHEJ.

The majority of clones from BLM or RTEL1 knockdown cells also had an intact *I-Sce*I site; however, structures indicating other repair processes were observed in 11 of 34 clones from BLM knockdown (*P* <0.0001 compared to NT) and 24 of 133 clones from RTEL1 knockdown cells (*P* = 0.0007). In four of BLM knockdown clones and 14 of the RTEL1 knockdown clones the entire 3-kb *copia* spacer sequence was copied from the repair template into the upstream *mCherry* (**Fig. 7B and 7C**). This extensive repair synthesis might occur through multiple cycles of strand exchange, as is believed to occur in *Drosophila* gap repair by SDSA (McVey et al, 2004), or through a single, continuous synthesis event. Among the 17 examples in which the entire spacer was copied, one from each knockdown sample had lost *neo^R*, a structure that is most consistent with a dHJ being resolved to give a crossover (**Fig. 7C**). The other 15 may have arisen by long-tract SDSA or by dissolution or non-crossover resolution of a dHJ (**Fig. 7B**).

There were additional repair events from knockdown cells that also had evidence of long-tract synthesis. Three events from BLM knockdown and seven from RTEL1 knockdown had a subset of the spacer copied into the upstream *mCherry* (**Fig. 7D**). These are most likely hybrid repair that involved long-tract synthesis followed by end joining. There was one event from the BLM knockdown that had an intact *I-Sce*I site but had lost *neo* (**Fig. 7E**). The source of this event and whether it occurred following *I-Sce*I cleavage is unknown.

BLM helicase does not alter cell cycle phases

Double-strand break repair pathway choice is believed to be dependent on the phase of the cell cycle; NHEJ preferred in G1 and HR favored in S/G2/M where a sister chromatid is available as a repair template. Detailed studies of the cell cycle progression coupled with DSBR assays in human cells indicate that although HR is dominating over S-phase it decreases in G2/M (Mao, 2008). NHEJ levels, however, are high throughout the cell cycle with the maximum at G2/M. To assess whether BLM helicase knockdown affects the cell cycle and thus could account for an increase in SDSA levels, I analyzed cell cycle profiles over the course of three days after BLM siRNA treatment and a non-targeting control (**Fig. 8**). The results indicate that BLM knockdown does not affect cell cycle and thus the SDSA increase in BLM-deficient cells is due to the BLM processing recombination intermediates rather than a chance in cell cycle phases.

	siRNA treatment		media change		adv-ISceI treatment		I-SceI cutting/ DNA repair	
	NT-Day 0	BLM-Day 0	NT-Day 1	BLM-Day 1	NT-Day 2	BLM-Day 2	NT-Day 3	BLM-Day 3
G1	74.9	75.3	44.1	47.1	35.1	38.5	40	38.2
S	16.2	16.4	38	33.5	49.2	47.35	45.2	46.7
G2	8.9	8.35	17.8	19.35	15.7	14.1	14.7	15.1
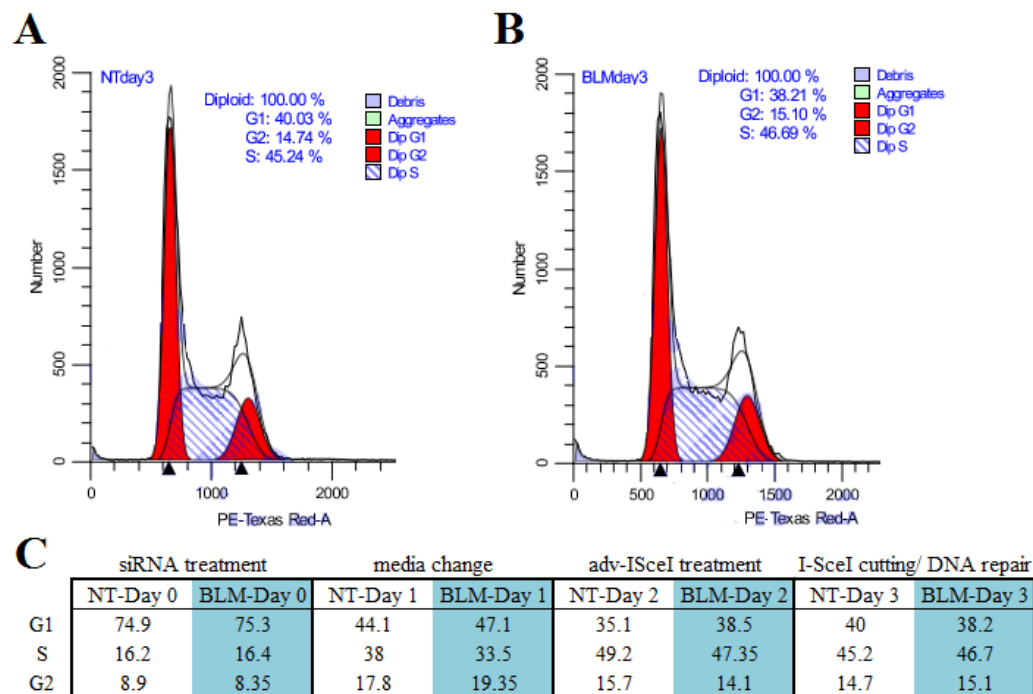
Figure 8. BLM helicase does not regulate the cell cycle phases.
Flow cytometry analysis of the cell cycle progression upon siRNA treatment in U2OS-SDSA cells. Flow cytometry graph representing DNA content upon propidium iodine staining in (**A**) NT siRNA Day 3 and (**B**) BLM siRNA Day3. (**C**) A table containing the percentage of cells in each phase of the cell cycle upon siRNA treatment measured every day for 3 days as indicated.

Small particle ML216, BLM inhibitor, affects SDSA

To gain further insights into the function of BLM helicase in SDSA, especially in regards of its inhibitory effects on SDSA revealed by the siRNA knockdown, I decided to test the effects of ML216 on the DSBR repair in U2OS-SDSA cells. ML216 is a small particle discovered in a large screen for BLM inhibitors (Nguyen and Hickson, 2013). Molecularly ML216 is a DNA mimicking compound with two aromatic rings that prevents BLM helicase from interacting with DNA. The authors of the paper characterized ML216 thoroughly using both biochemical and genetic approaches. 50 uM concentration of ML216 inhibits DNA binding and the helicase activity of both truncated and full-length BLM. Gel-based DNA unwinding assays reveled that ML216 is inhibiting primarily BLM and at higher doses can also inhibit WRN helicase, but no inhibition was discovered for other RecQ helicases like RecQL1, RecQL5, and URVD. BLM deficient cells exhibit high levels of SCEs (Wechsler et al., 2011) ML216 mimics this phenotype but to a lesser degree, however, it does not exacerbate the elevated SCE phenotype in the cells already devoid of BLM (Nguyen and Hickson, 2013). To assess the influence of ML216 on SDSA in human cells, I treated the cells with the inhibitor at the same time when I-SceI-expressing virus was added. Surprisingly, ML216 treatment leads to a two-fold reduction of SDSA frequency (**Fig 9A**) as oppose to a two-fold increase of SDSA in BLM siRNA knockdown (**Fig 5A**).

The striking contrast between ML216 and BLM siRNA phenotypes indicates that ML216 might have other, yet unknown, targets in the cell that are necessary for SDSA, or that ML216-bound and deactivated BLM is now binding and sequestering other DSB repair proteins preventing them from executing SDSA. To parse out which of these two aforementioned effects

28

ML216 might have on the cell, I designed an experiment in which the cells are transfected with BLM siRNA prior to ML216 treatment. If ML216 acts on BLM helicase then knocking down BLM should render ML216 ineffective and thus SDSA levels will go up. However, if ML216 has a different target, then the ML216 phenotype will supersede the one of BLMs, and the SDSA levels will go down. The data of the ML216 treatment in conjunction with the siRNA transfection (**Fig. 9B**) indicate that ML216 is likely targeting a different DNA DSBR protein target other than BLM helicase as the SDSA levels are reduced even in the cells treated with BLM siRNA. It is worth noting that, although ML216 can inhibit WRN helicase, there must be other ML216 targets in the cell affecting SDSA since WRN knockdown does not affect SDSA (**Fig 5A**).
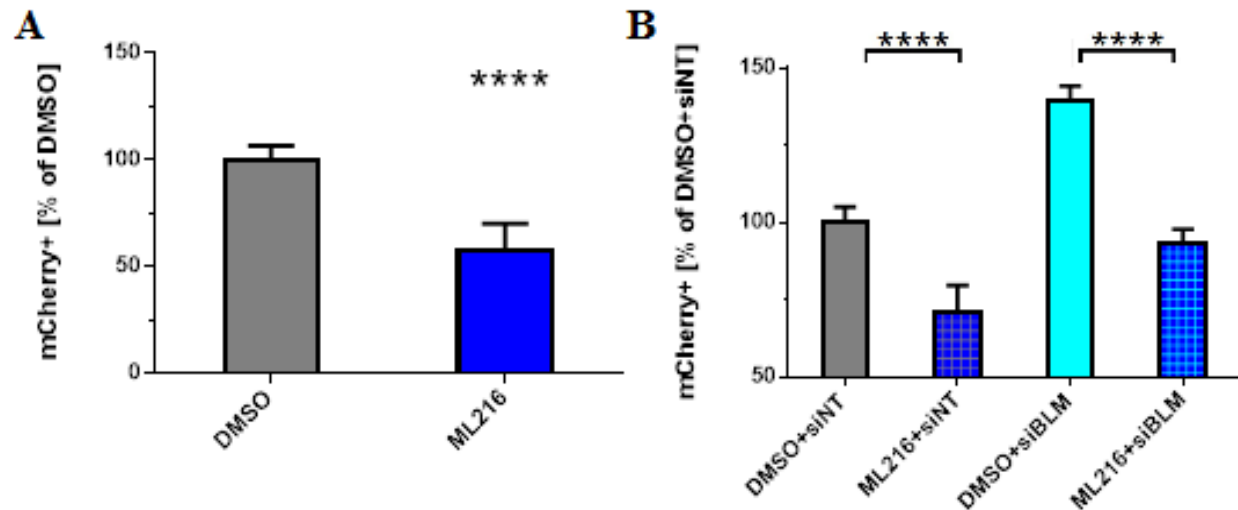
Figure 9. BLM inhibitor, ML216, influences SDSA.
(**A**) Relative SDSA frequency in SDSA-U2OS cells upon ML216 treatment. X-axis: different drug treatments; Y-axis: percent of the cells exhibiting mCherry fluorescence; values: averaged results of 5 experiments with 14 data points per treatment; error bars: standard deviation; significance: ML216 vs.DMSO: ****; $p < 0.0001$.
(**B**) Relative SDSA frequency in SDSA-U2OS cells upon ML216 and siRNA treatment. X-axis: different drug and siRNA treatments; Y-axis: percent of the cells exhibiting mCherry fluorescence; values: averaged results of 3 experiments with 8 data points per treatment (DMSO-siNT and ML216-siNT) and 1 experiment with 4 data points (DMSO-siBLM and ML216-siBLM); error bars: standard deviation.

BLM helicase is a negative SDSA regulator in HeLa cells

To complement the research I have conducted in U2OS and to investigate whether SDSA

regulation is specific to U2OS or universal across all human cell, I repeated some of the

aforementioned experiments in HeLa cells. First, I stably integrated linearized pSDSA into HeLa

cells and upon infection with the *I-Sce*I- expressing virus, I observed mCherry positive cells

under the fluorescent microscope (**Fig. 10A**). Then, I tested the consequences of BLM

knockdown for SDSA regulation (**Fig. 10B**). BLM helicase in HeLa cells, just like in U2OS, is a

negative SDSA regulator, indicating that the roles of DNA helicases in all human cells are

conserved.
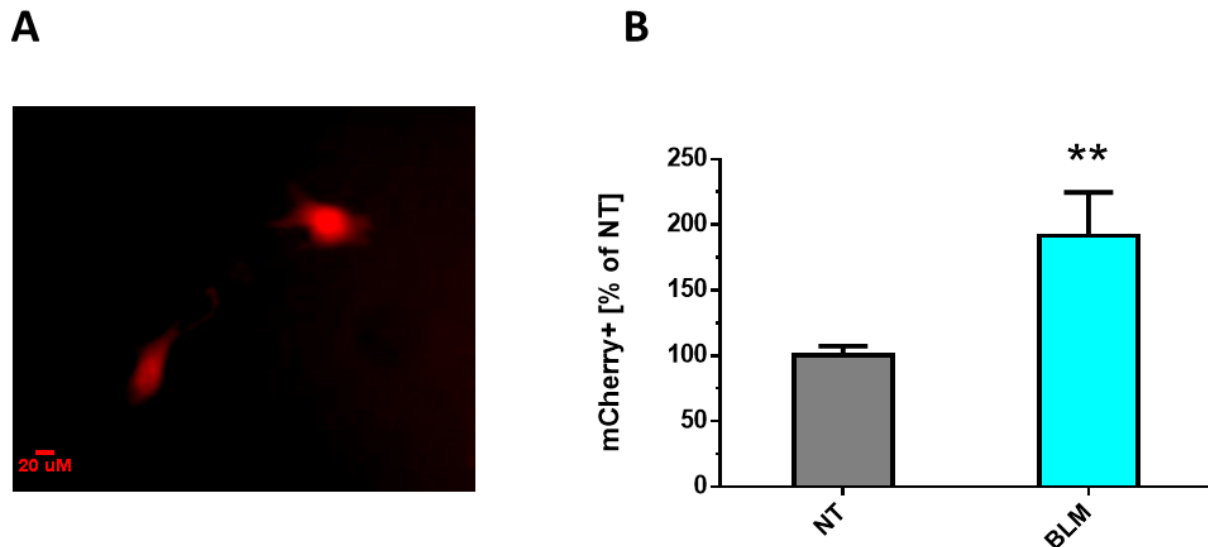
Figure 10. BLM helicase is a negative SDSA regulator in HeLa cells.
(**A**) Fluorescence microscopy image of mCherry positive HeLa cells. (**B**) Relative SDSA frequency in
SDSA-HeLa cells upon siRNA treatment. X-axis: different siRNA treatments; Y-axis: percent of the
cells exhibiting mCherry fluorescence; values: averaged results of 3 experiments with 4 data points per
treatment; error bars: standard deviation; significance: NT vs. BLM: ** $p=0.0017$.

Conclusion

In conclusion, I showed that human cells, as hypothesized, can utilize SDSA to repair DSBs. I developed the first human cell SDSA assay, which is a tool designed specifically to detect SDSA in human cells by following mCherry fluorescence using flow cytometry (**Fig. 2** and **Fig. 4**). I also identified two helicases, BLM and RTEL1, which are SDSA regulators in human cells (**Fig. 5**). Unlike our initial hypothesis based on the results derived from yeast and fruit flies, BLM and RTEL1 do not promote SDSA, but rather are its negative regulators, which I demonstrated by utilizing an siRNA knockdown approach targeting various helicases (**Fig 5**). I observed a nearly two fold increase (on average from 1.4% to 2.4%) in SDSA efficiency in the cells devoid of BLM or RTEL1 (**Fig 5**). I also determined that these helicases, despite their multiple functions in the DSBR pathway and in the cell, act in a BRCA2-dependent manner (**Fig. 6**), which means that the SDSA regulation occurs post the homology search step in the DSBR model (**Fig 1**).

To further investigate the contribution of BLM and RTEL1 to double-strand break repair, I analyzed single-cell derived colonies of the siRNA treated repair events at the molecular level (**Fig 2** and **Fig. 7**). All mCherry positive clones are SDSA events as determined by sequencing and resistance to I-SceI cutting (**Fig. 2**). mCherry negative clones from the BLM and RTEL1 siRNA treated cells exhibit various repair patterns (**Fig. 7**) indicating that they can be a result of SDSA, DSBR with dHJ resolution or dissolution, NHEJ, or a combination of the above; SDSA followed by DSBR or end-joining.

Comprehensive molecular analysis indicates that the synthesis-tract length is extended in the helicase-deficient background which can account for observed SDSA increase. Regardless, I explored other possibilities in attempt to investigate the increased SDSA phenotype in siBLM

31

samples. I conducted a series of SDSA assay experiments using BLM inhibitor – ML216, which unexpectedly revealed that ML216 treatment decreases SDSA efficiency in a BLM-independent manner indicating that ML216 has another target in the cell. (**Fig. 8**). Lastly, I performed a detailed cell cycle analysis to reveal whether BLM helicase extends S-phase and thus promotes HR, but I did not find any evidence to support it.

Together, the data from Chapter 2 confirm that SDSA is a major pathway of DSBR in human cells and that DNA helicases, such as BLM and RTEL1, regulate it. DNA helicases are also thought to inhibit hyper-recombination by limiting the number of COs in mitotically dividing cells. A dramatic increase in HR in the cells with reduced BLM or RTEL1 levels supports that notion. To attempt answering questions regarding the contribution of DNA helicases to CO regulation, I designed a fluorescence based CO-GC assay. The experimental approached successfully utilized in Chapter two has been instrumental in learning about SDSA in human cells. I used a similar approach when looking at COs and GCs in human cells, which I discuss in Chapter 3.

Materials and Methods

Construction of assay plasmids

The SDSA assay construct was based on pEF1a-mCherry-C1 vector (Clonetech #631972). A fragment of *mCherry* was removed by cutting with *Nhe*I and *Hin*dIII and inserting annealed oligonucleotides containing an *I-Sce*I recognition sequence and a part of the *mCherry* sequence. The product, pEF1a-mCherry-I, had 350 bp of *mCherry* deleted and the *I-Sce*I sequence inserted. In parallel, 5' and 3' mCherry fragments, overlapping by 350 bp, were PCR-amplified and cloned into a vector containing a fragment of the *copia* retrotransposon from *D. melanogaster*. A fragment of *HPRT* was cloned out of the DR-GFP construct. This entire module (5' *mCherry – copia – 3' mCherry – HPRT*) was PCR-amplified and cloned into the pEF1a-mCherry-I to produce pSDSA.

Generation of stably transfected cell lines

U2OS and HeLa cells were cultured under normal conditions (DMEM +10% FBS + pen/strep) for 24h till they reached 80% confluency before transfection with the SDSA assay constructs using a Nucleofector™ 2b Device (Lonza #AAB-1001) and Cell Line Nucleofector® Kit V (Lonza #VCA-1003). One week post-transfection appropriate antibiotics were added to select for the cells with a stably-integrated construct. The SDSA assay construct contains a neo^R gene; cells receiving this construct were treated with 700 μg/ml G418 (Sigma # A1720) for one week and then a single-cell clones were derived.

DNA repair assay and flow cytometry

SDSA-U2OS cells were cultured in 10 cm dishes containing 10 ml of DMEM medium with high glucose; Corning) until split onto 6-well plates at a concentration of 5×10^4 cells per milliliter using 0.05% Trypsin 0.53% mM EDTA solution (Corning). Upon reaching ~60% confluency, the cell were treated with an siRNA reaction mixture (90 nmol of siRNA and 8 µl lipofectamine 2000 reagent per well; Invitrogen). 24 hours after transfection the siRNA reaction mixture was replaced with the fresh culture medium. 12 hours later the cells were treated with 100 µl of *I-Sce*I-expressing adenovirus (Anglana and Bacchetti, 1999) (previously titrated to a non-lethal concentration). After another 24 hours the medium was replaced and thus the adenovirus removed. 72 hours later the cells were harvested and resuspended in 1x PBS (Corning) supplemented with 2% fetal bovine serum (FBS) and 5 mM EDTA for flow cytometry acquisition on a BD LSRFortessa, using 488nm and 561nm lasers to detect the mCherry fluorescence.

Genomic DNA isolation

Cells were cultured in a 15 cm dish till they reached 100% confluency. Then they were rinsed gently with 1x PBS and harvested using 0.05% Trypsin 0.53 mM EDTA and pelleted by centrifuging for three minutes at 2000 rpm. Cells were washed with PBS and transferred to 1.5ml microfuge tubes and spun for 10 sec to re-pellet. PBS was removed and cells were resuspended in TSM + 0.5%NP-40 solution (140 mM NaCl; 10 mM Tris-HCl, pH 7.4; 1.5 mM $MgCl_2$), then incubated on ice for 2-3 minutes. After pelleting, cells were resuspended in 1 ml nuclei dropping buffer (0.075 M NaCl; 0.024 M EDTA, pH 8.0). The suspension was transferred to a 15 ml tubes containing 4 ml of nuclei dropping buffer with 1mg of Proteinase K (final Proteinase K

34

concentration = 0.2 mg/ml), and 0.5% of SDS. The cells were lysed overnight at 37°C. The next day an equal volume of phenol was added to lysed nuclei and mixed on an orbital shaker for two hours followed by a five minute spin at 2000 rpm. The aqueous phase was transferred to a clean tube and an equal volume of chloroform was added and the mix was incubated for 30 mins on an orbital shaker. After spinning, the aqueous phase was transferred to a new tube and 0.1 volumes of 3M sodium acetate was added, followed by one volume of isopropanol. The DNA was spooled out using a glass Pasteur pipette and resuspended overnight in 1 ml TE buffer (10 mM Tris-HCl, pH 8.0; 1 mM EDTA, pH 8.0). The next day the DNA was precipitated using 0.5 volumes of 7.5M NH_4OAc and two volumes of ethanol. DNA was spooled out and resuspended in 0.5ml TE-4 buffer (10mM Tris-HCl, pH 8.0; 0.1mM EDTA, pH 8.0). Samples were stored in 4°C until analyzed.

PCR analysis of the repair events

DNA from the repair events was isolated according to the protocol above and used in a PCR reaction to amplify a desired DNA fragment for sequencing or fragment length characterization. 1.5ul DNA was added to each PCR mixture containing primer sets according to the Table 2, iProof polymerase (BioRad #424264), and a buffer. PCR amplification reaction program was 33 cycles of [20s-98°C; 20s-64°C; 20 to 150s-72°C]. The PCR products were run on a 1-1.5% agarose gel with EtBr before imaged.

Table 2. PCR primers used in the SDSA assay study and their location

	primer	sequence	amplicon size [bp]
1.	neo_F	ggatgaggatcgtttcgcatg	996
2.	neo_R	catagaaggcggcggtggaatcg	
3.	nheI_F	cgtgacgctagcgctaccgg	433 if intact I-SceI
4.	hindiii_R	cgaagcttgagctcgagatc	783 if SDSA
5.	pSDSAprom_F	ggccaagatctgcacactgg	↓
6.	SDSAseq1_R	cctcgcagcaaatgctggatc	1298
7.	SDSAseq2_R	cagagaatcaactggctgac	1498
8.	SDSAseq3_R	cgtgagagaagctctatggc	1707
9.	SDSAseq4_R	ctgtgggcctattactccag	2640
10.	SDSAseq5_R	gtcccacgcgtcgacaaggc	4112
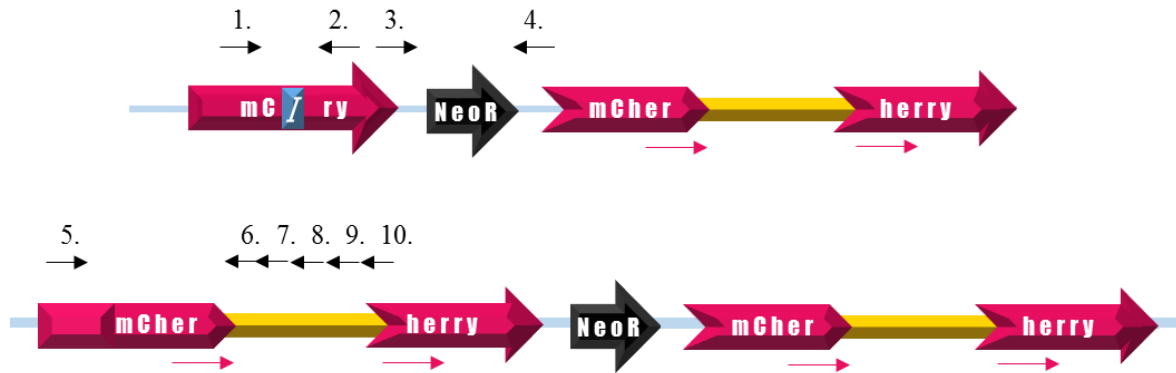
Western blot of BLM protein siRNA-treated cells

U2OS cells were transfected using *BLM* siRNA or NT siRNA (90nmol) and lipofectamine 2000 (8 μl; Invitrogen) and harvested on the third day post-transfection using 0.05% Trypsin 0.53% mM EDTA solution (Corning). After washing with 1x PBS the cells were resuspended in a protein sample buffer (Tris-HCl; SDS; glycerol; bromophenol blue; 150mM DTT) and boiled. 20 μl of the protein sample was loaded on a 7.5% SDS-PAGE gel and the gel was run for 1-2 hours at 100V. Protein was transferred to a PVDF membrane using a wet transfer method (1.5 h at 90 V in 4°C). The membrane was blocked in 5% milk PBS solution and

incubated in PBS plus 0.1% Triton-X plus primary antibodies (rabbit anti-BLM [Abcam #2179] at 1:2000 and mouse anti-αTubulin [Sigma #T9026] at 1:8000) overnight at 4°C, rocking. The membrane was then washed three times in PBS-T solution. HRP-conjugated secondary antibodies were added (goat anti-rabbit 1:5000; goal anti-mouse 1:100,000) and the blot was incubated for 1 hour at room temperature. The membrane was washed three times in PBS-T solution and then incubated in an ECL solution (Thermo Fisher) for chemiluminescence for two minutes. The Western blot image was taken using BIO-RAD Molecular Imager (ChemiDoc XRS+) or the X-ray film was developed using a developer.

qPCR evaluation of the siRNA knockdown efficiency

U2OS cells were transfected using desired siRNA (90 nmol) and lipofectamine 2000 (8 μl; Invitrogen) and harvested on the 3rd day post-transfection using 0.05% Trypsin 0.53% mM EDTA solution (Corning). RNA was extracted using a manufacturer's protocol for ReliaPrep RNA Cell Miniprep System (Promega). Purified RNA was used as a template to generate cDNA library with QuantiTect Reverse Transcription Kit (Qiagen # 205310). The qPCR mix was contained gene-specific DNA primers, cDNA, and QuantiTect SYBR Green PCR kit (Qiagen #A 204141). Amplification and quantification was conducted on a RealTime PCR machine (QuantStudio 6 flex Real Time PCR System).

Cell cycle analysis by DNA content using propidium iodide

U2OS-SDSA cells were washed by centrifugation (200 x g, 5 min, 4°C) two times in protein-free buffer Phosphate Buffered Saline without Ca+2 or Mg+2 (PBS). The cells were resuspended at 2×10^6 cells in 1 ml of ice cold PBS buffer. Cell number will effect staining.

Then the cells were vortexed gently, and then the cell suspension was added dropwise to 9 ml of 70% ethanol in a 15 ml polypropylene centrifuge tube (Falcon® Cat. No. [35]2097). Cell precipitation was observed with a microscope to verify minimum cell clumping. The cells were stored at 4°C for 12 - 24 hours before the propidium iodide stating. The cells were centrifuged at 200 x g, 10 min, 4°C, and the pellet resuspended in 3 ml of cold PBS and transferred to Falcon® 12 X 75 mm (Cat. No. [35]2054) polystyrene tubes for staining Falcon® Cat. No. [35]2235. The cell were resuspended in 300 - 500 µl PI/Triton X-100 staining solution: 10 ml of 0. 1 % (v/v) Triton X-100 (Sigma) in PBS add 2 mg DNase-free RNase A (Sigma) and 0.40 ml of 500 µg/ml PI (Roche # 11348639001). The cells were incubate 37°C for 15 minutes or for 30 min at 20°C, then stored at 4°C. The data was acquired on a BD LSRFortessa flow cytometer and analyzed using ModFit LT version 4.1 by Verity Software House.

Statistical data analysis

GraphPad Prism 6 software (version 6.07) was utilized to generate the figures presenting the flow cytometry results of the SDSA assay. Prism also provides a statistical data analysis platform. The data was analyzed using two statistical tests; one-way ANOVA with a correction for multiple comparisons or Student T test if a single comparison was needed.

CHAPTER 3

CROSSOVERS AND GENE CONVERSIONS IN HUMAN CELLS

Introduction

Over a 100 years ago Thomas Morgan published his work describing chromosomes as the units of inheritance and proposed crossovers as a mechanism for unlinking genes and generating diversity during reproduction (Morgan et al., 1915). The first experimental evidence however, came from the studies conducted by Barbara McClintock on crossing *Zea mays* and analyzing recombinant progeny (Creighton and McClintock, 1931). Over 50 years ago Robin Holliday proposed a model in which the main recombination intermediate is a structure of two interconnected DNA helices that he called a Holliday junction (HJ) (Holliday, 1964). However, according to the most frequently cited model for HR, DSB processing generates not a single but double HJ (dHJ) (Szostak et al., 1983), which needs to be cleaved for proper chromosomal segregation during cell division. HJs are cleaved by specialized endonucleases, called resolvases, to generate either a reciprocal crossover (CO; **Fig. 1E**) or a noncrossover (NCO; **Fig. 1E'**). Either can be associated with gene conversion, in which the exchange of genetic material is unidirectional (Szostak et al., 1983). COs in meiotically dividing cells are programmed and desired as they prevent chromosomal non-disjunction that could lead to chromosome number alterations like in Down syndrome. Genetic diversity is also a result of dHJ processing into COs. In proliferating cells, in particular, crossovers between homologous chromosomes are not desired because they may lead to loss of heterozygosity (LOH) (LaRocque et al., 2011; Wang et al.,

2011) and chromosome rearrangements in cases of ectopic recombination between DNA duplications (Liu et al., 2011). LOH has been implicated in carcinogenesis as it leads to the loss of functional copies of tumor suppressor genes (Bignon, 2004; Knudson, 1971; Luo et al., 2000).

Although the high level of SCEs is a cellular hallmark of BLM-deficient cells, crossovers between sister chromatids do not explain propensity for mutations and cancer development in Bloom syndrome patients (Chaganti et al., 1974; Wechsler et al., 2011). These symptoms can be explained however if elevated levels of COs between homologous chromosomes leading to LOH are present. Studies of LOH point out to BLM helicase as one of the important players preventing recombination (LaRocque et al., 2011). In the S/P assay developed by Jeannine LaRocque in ES cells, LOH is measured after introducing a DSB in two allelic neo^R genes residing on homologous chromosomes. The loss of polymorphisms between the two neo^R alleles resulting from a CO conversion or a NCO conversion constitutes LOH. BLM-deficient cells exhibit 12.9% of LOH while the control cells - less than 2.5%. Interestingly, in the control experiment all LOH events came from NCO conversion, while in the BLM-deficient cells the majority came from the CO conversion.

In Chapter 2, I showed the development of the first SDSA assay in human cells and that DNA helicases such as BLM and RTEL1 are important SDSA regulators. The molecular analysis data indicate that BLM and RTEL1, despite negatively controlling SDSA, still act as recombination inhibitors (a dramatic elevation of HR in helicase knockdown cells). This raises questions about the contribution of helicases to CO and GC regulation. This chapter is dedicated to the GC analysis conducted using DR-GFP assay and the development of a novel CO-GC assay in human cells using DR-GFP as a backbone.

Results

Gene conversion regulation in human cells using DR-GFP assay

DR-GFP, although initially developed in the Jasin laboratory (Pierce et al., 1999) in ES cells, quickly became a golden standard in studying HR and was adapted for human HEK293 and U2OS cells (Paliwal et al., 2014; Wang et al., 2011). In this assay a DSB is generated by introducing a source of I-SceI to cut a non-functional *GFP* gene (**Fig. 11A**). DSB can be repaired using a downstream template, *iGFP*, which will restore a functional *GFP* gene (**Fig. 11B**). The restoration of a functional *GFP* can occur via SDSA and is often interpreted as such, however it can also occur via dHJ dissolution or resolution with the repair template on the homologous chromosome. CO between the upstream *GFP* gene and the downstream template is also possible, although will not generate a functional *GFP* due to *iGFP* repair template missing the *GFP* 3'end sequence as indicated in Fig. 11B, and would lead to a deletion of the intervening sequence. The same rationale applies to a possible SSA repair which would not result in the restoration of the functional GFP gene.
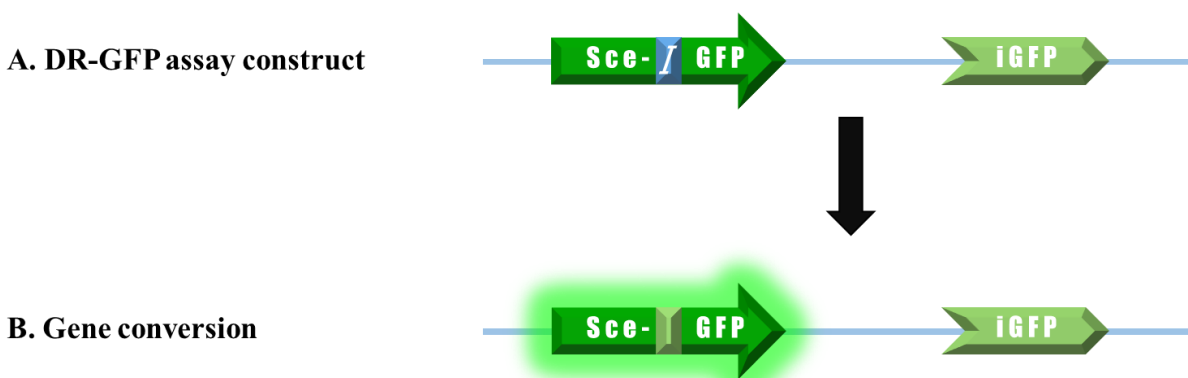
Figure 11. DR-GFP assay design.
(**A**) DR-GFP assay construct consisting of two non-functional *GFP* genes: upstream GFP with an I-SceI recognition sequence where the DSB is going to be generated; downstream iGFP that shares a homology to the sequence surrounding the I-SceI cut sire, but is missing both 5' and 3' GFP end necessary to constitute a functional *GFP* gene. (**B**) A product of a DSB repair with a GC outcome leading to a restoration of the functional *GFP* gene.

Paliwal *et al* in 2014 made an attempt to find a human functional ortholog of yeast Srs2 and tested a number of helicases using DR-GFP assay using an siRNA approach (Paliwal et al., 2014). They revealed RECQL5 knockdown lead to a decrease in GC in both HEK293-DRGFP and U2OS-DRGFP cells. This function of RECQL5 was BRCA1-depedant and thus they proposed that RECQL5 dismantles aberrant Rad51 filaments that prevent SDSA. Surprisingly, RECQL5 depletion drastically reduced an elevated level of NCOs in BLM-depleted HEK293 cells (the results for U2OS were not reported). Another candidate for Srs2 human ortholog, hFBH1 helicase (FBXO18), was also tested and surprisingly FBH1 depletion lead to two-fold increase in GCs levels, but only in U2OS cells and not HEK293.

To assess the function of these, and other helicases in U2OS, I performed an experiment utilizing siRNA knockdown of BLM, FBXO18, FANCM, RECQL5, RTEL1, and BRACA2 as a control (**Fig 12A**). As mentioned in Chapter 2, BRCA2 is necessary for RAD51 loading and homology search. BRCA2 depletion in U2OS-DRGFP cells leads to a three-fold decrease in GFP fluorescence, indicating CGs in this assay are DNA 3'-end invasion dependent. Only depleting FANCM helicase leads to a decrease in GC levels in U2OS. However, depleting FBXO18 and RTEL1 leads to a moderate but significant increase in GCs. GC increase in FBXO18 is consistent with the previously published results (Paliwal et al., 2014; Wang et al., 2011), and the increase in RTEL1 GC levels is not surprising, considering RTEL1 depletion leads to a two-fold increase in SDSA as well (**Fig. 5A**). RECQL5 depletion did not lead to a change in GCs levels, unlike reported before, perhaps due to differences in the experimental design or I-SceI delivery (viral infection vs plasmid transfection). BLM depletion leads to a high level of cell death which could explain why the GC levels in U2OS-DRGFP cells remained unchanged, unlike reported in HEK293, or it is a bone-fide difference between U2OS and HEK293 cells.
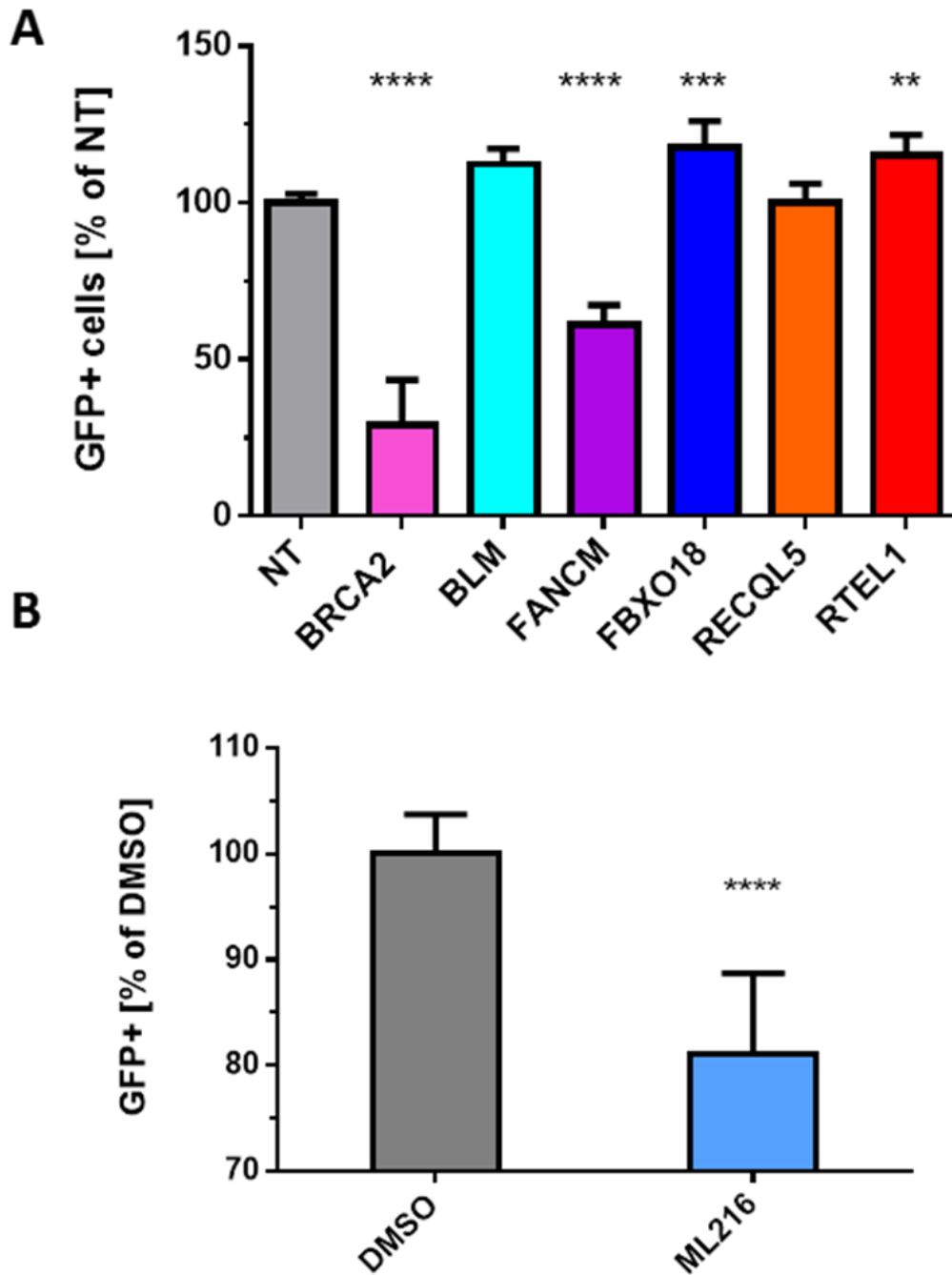
Figure 12. DNA helicases regulate gene conversion levels in U2OS.
(**A**) Relative GC frequency in DRGFP U2OS cells upon siRNA treatment. X-axis: different siRNA treatments; Y-axis: percent of the cells exhibiting GFP fluorescence; values: averaged results of 2 experiments with 8 data points per treatment (except BLM: 4 data points due to poor viability); error bars: standard deviation; BLM statistically significant using Student T test, but not Anova analysis for multiple comparisons. (**B**) Relative GC frequency in U2OS-DRGFP cells upon drug treatment. X-axis: different drug treatments; Y-axis: percent of the cells exhibiting GFP fluorescence; values: averaged results of 2 experiments with 8 data points per treatment; error bars: standard deviation.

In addition to the siRNA approach, I performed an experiment with ML216; a small particle identified as BLM inhibitor (Nguyen and Hickson, 2013). GCs in the U2OS-DRGFP cells treated with ML216 are significantly reduced (**Fig. 12B**) but not to the same degree as they were in U2OS-SDSA (**Fig. 9A**). The exact mechanism of ML216 action and if BLM helicase is the only target remains unclear.

Development of the Crossover-Gene conversion assay

One limitation of the DR-GFP assay is it does not allow to determine whether GCs are associated with COs, if they are a product of dHJ dissolution, or SDSA. The development of the SDSA-specific assay was described in Chapter 2. To determine which GCs are associated with COs and which are not, I designed a novel CO-GC assay using the same principles DR-GFP assay was built on (**Fig. 13A**). The CO-GC assay consists of a non-functional, I-SceI-interrupted *GFP* gene where the DSB is going to be generated; the repair template which is a non-functional *iGFP* gene with a 5'-end deleted; a functional mCherry gene. The *iGFP* gene is placed in the intron of the *mCherry* gene in the opposite orientation to the upstream *GFP* gene. The cells stably transfected with the linearized CO-GC assay construct will exhibit red fluorescence from the functional *mCherry* gene (**Fig. 13A** red glowing arrow). Upon introduction of the source of I-SceI, the gap will be repaired off of a downstream *iGFP* gene. GC without a CO will lead to a restoration of the functional *GFP* gene and the cell will gain green fluorescence in addition to the red fluorescence deriving from mCherry (**Fig. 13B**). GC with a CO will lead to a sequence inversion between the two *GFP* genes due to their opposite orientation (**Fig. 13C**). Because the *iGFP* repair template is located in an intron of the *mCherry* gene, a CO-initiated inversion will cause a separation of the mCherry promoter, which is distal to the repair template, from the

44

mCherry open reading frame, which is proximal to *iGFP* rendering *mCherry* nonfunctional. The cells will lose red fluorescence and turn green. The positioning of the two *GFP* genes ensures no SSA repair can occur.
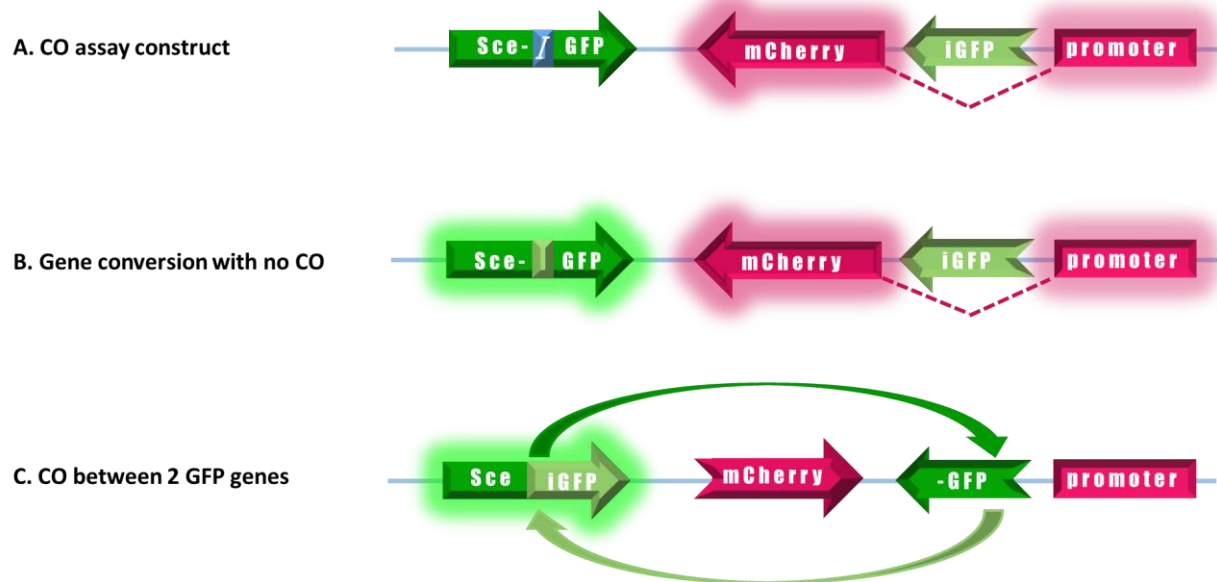
Figure 13. Human CO assay design.
(A) Human CO assay construct consisting of: nonfunctional *GFP* gene (dark green arrow) interrupted by the *I-Sce*I recognition sequence (the site of the DSB once the source of I-SceI is introduced; White letter "I" on a blue background); functional *mCherry* gene (pink arrow) with its promoter (pink box); *iGFP* gene (light green arrow) inserted into mCherry intron sequence in an opposite orientation to the nonfunctional *GFP* gene. The cells exhibit mCherry fluorescence only; **(B)** CO assay construct after the occurrence of a gene conversion without CO. A functional GFP gene is restored. The cells exhibit both GFP and mCherry fluorescence; **(C)** CO assay construct after a CO between 2 GFP genes. The functional GFP gene is restored but the inversion between the 2 *GFP* genes lead to a separation of the mCherry gene from its promoter sequence leading to mCherry disruption. The cells exhibit GFP fluorescence only.

To generate cell lines with the CO-GC assay construct, I transfected U2OS and HEK293 cells with a linearized pCO-GC vector and used puromycyn to select stably-integrated lines. To induce DSBs, I infected U2OS CO-GC cells with an adenovirus expressing *I-Sce*I (Anglana and Bacchetti, 1999) and HEK293 CO-GC cells with the *I-Sce*I expressing vector (Pierce et al., 1999). The adenovirus undergoes a lytic cycle in HEK293 cells which are used to multiply the

virus, therefore these cells are not suitable with the I-SceI adenovirus. I detected mCherry and

GFP activity in U2OS (**Fig. 14**), and HEK293 (**Fig. 15**) cells by fluorescence microscopy as

early as two days after viral infection. Furthermore, I utilized a flow cytometry approach to

quantify the number of cells in each fraction and determined the levels of COs and GCs (**Fig.**

14D).
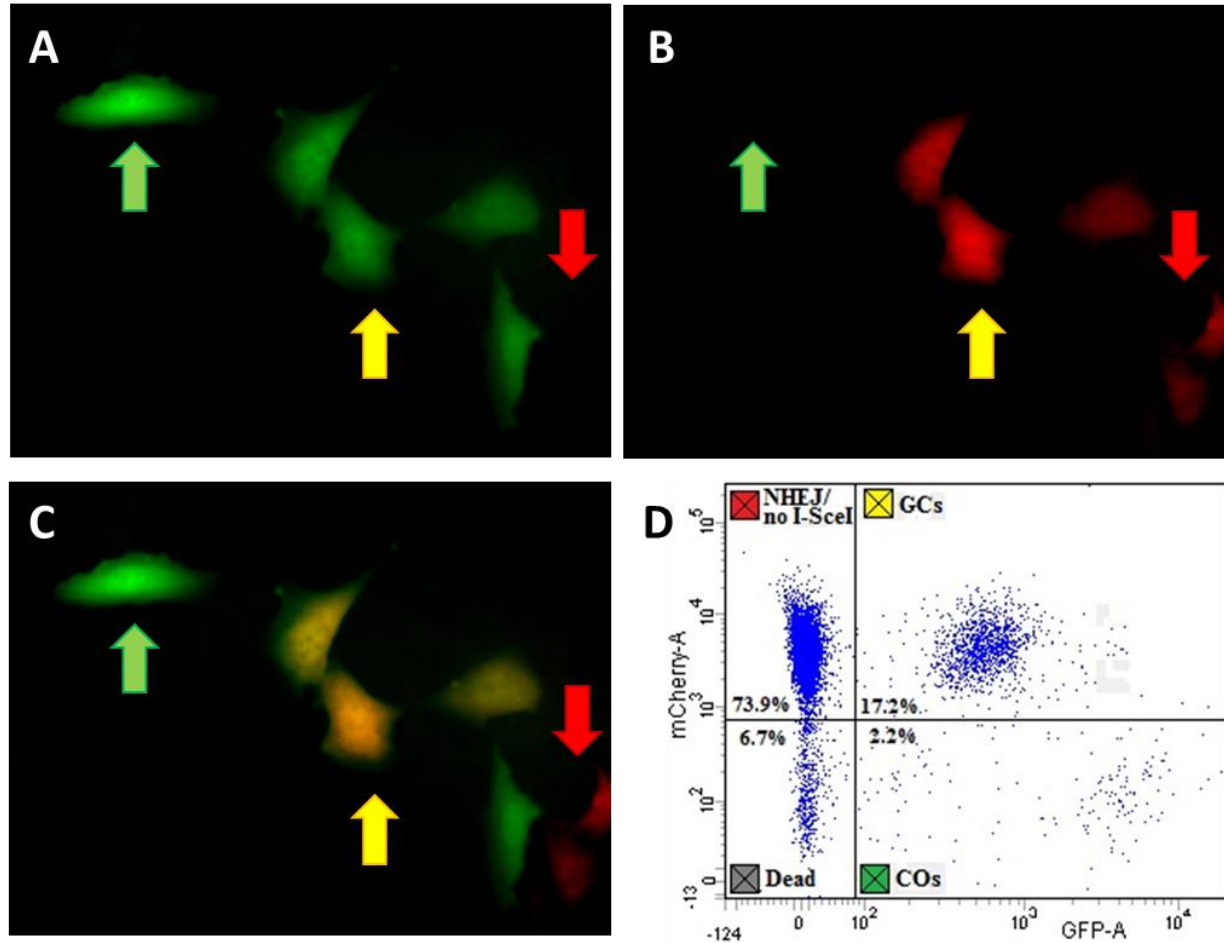
Figure 14. CO-GC assay in human U2OS cells.
(**A-C**) Fluorescent images of the U2OS cells two days after adeno-I-SceI infection. Red arrows mark the cells that underwent precise NHEJ/no I-SceI cutting events; Green arrows indicate cells that underwent a CO event; Yellow arrows mark the cells that underwent a GC event. (**A**) U2OS cells captured in the mCherry channel. (**B**) U2OS cells captured in the GFP channel. (**C**) Merged image of mCherry and GFP channels. (**D**) Flow cytometry graph with the level of GFP fluorescence on the x-axis and mCherry fluorescence on the y-axis. The percent of each cell population after I-SceI cutting as indicated.
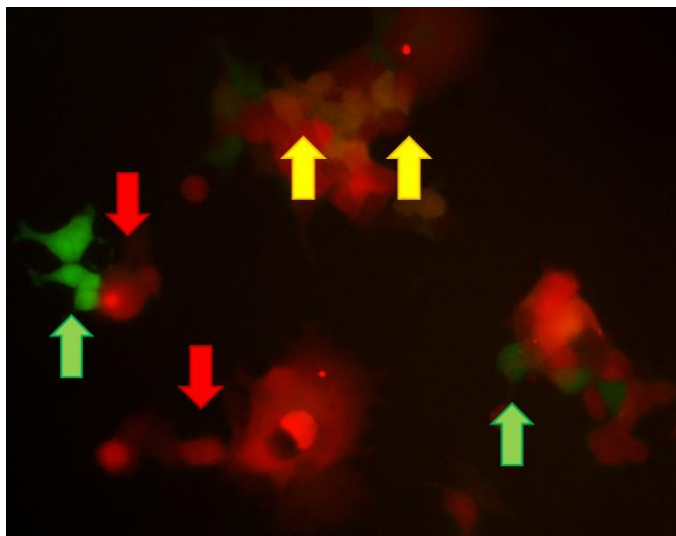
Figure 15. CO-GC assay in human HEK293 cells.
Fluorescent microscopy image of the HEK293 cells two days after nucleofection with the I-SceI expressing plasmid. Red arrows mark the cells that underwent precise NHEJ/no I-SceI cutting events; Green arrows indicate cells that underwent a CO event; Yellow arrows mark the cells that underwent a GC event. Merged image of the cells visible in mCherry and GFP channels.

BLM helicase prevents crossovers and gene conversions in U2OS

To assess the role of BLM in determining DSBR outcomes I utilized an siRNA approach and knocked down BLM helicase in U2OS CO-GC cells. BLM depletion has been shown to cause both: elevated levels of SCEs, a hallmark of COs (Wechsler et al., 2011), and increased GCs (Paliwal et al., 2014), but using different assays. The advantage of the CO-GC assay is the ability to investigate both of these outcomes at the same time and compare them to one another. BLM knockdown in U2OS CO-GC cells cause a dramatic increase in CO levels but only a moderate one in GCs (**Fig. 16**). Data interpretation beyond this point proved to be challenging due to the high experiment to experiment variation of the ratio between COs and GCs. Considering that revealing COs events requires not only a loss of the *mCherry* gene but also a sufficient mCherry protein turnover, precise quantification using a flow cytometer within a siRNA knockdown timeframe might require further optimization.

47
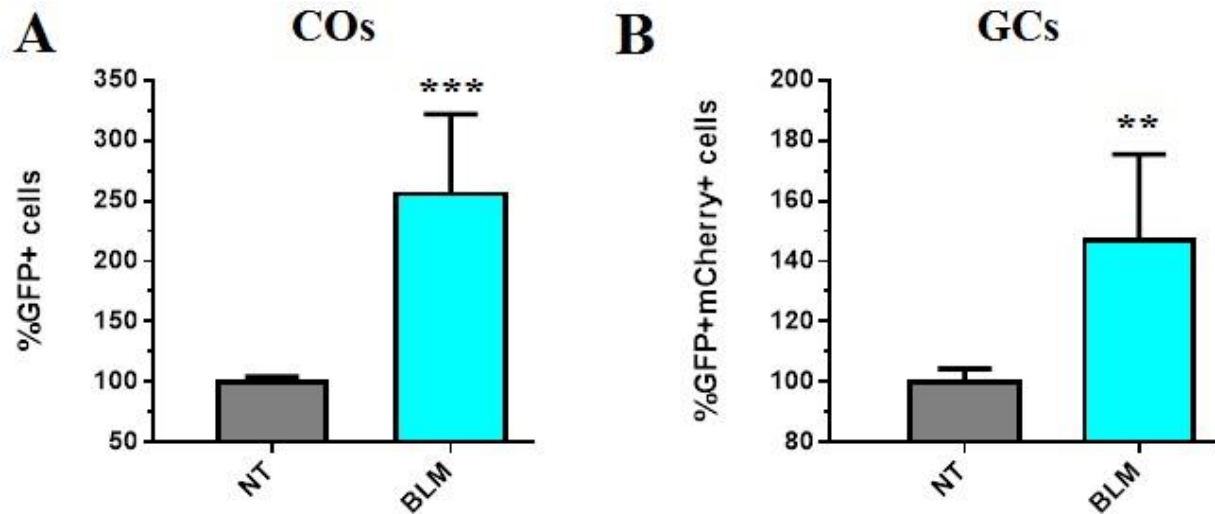
Figure 16. BLM helicase inhibits COs and GCs in U2OS CO-GC cells.
Relative CO and GC frequency in U2OS CO-GC assay cells upon siRNA treatment. X-axis: different siRNA treatments; **(A)** Y-axis: percent of the cells exhibiting GFP fluorescence; values: averaged results of 2 experiments with 5 data points per treatment; error bars: standard deviation; significance: $p=0.0008$. **(B)** Y-axis: percent of the cells exhibiting GFP and mCherry fluorescence; values: averaged results of 2 experiments with 5 data points per treatment; error bars: standard deviation; significance: $p=0.0066$.

BLM and FANCM prevent COs independently

Both BLM and FANCM helicases have been implicated in affecting numerous levels of the DSBR pathway such is D-loop disruption, SDSA regulation, prevention of CO outcomes (see Introduction). Because Bloom Syndrome and Fanconi Anemia patients share multiple phenotypes such as sensitivity to DNA damaging agents and predisposition to cancer it had been proposed these two helicases might act together in resolving DNA intrerstrand crosslinks or 3'-end resection (Suhasini and Brosh, 2012; Vinciguerra and D'Andrea, 2009). To assess the relationship between BLM and FANCM, I depleted either one of both helicases using siRNA approach in U2OS CO-GC cells and measured CO and GC levels (**Fig. 17**). The results indicate that BLM and FANCM depletion has an additive effect on CO levels but not on GC levels. This analysis is only preliminary as the experiment was conducted once due to flow cytometer repairs and availability issues.

48
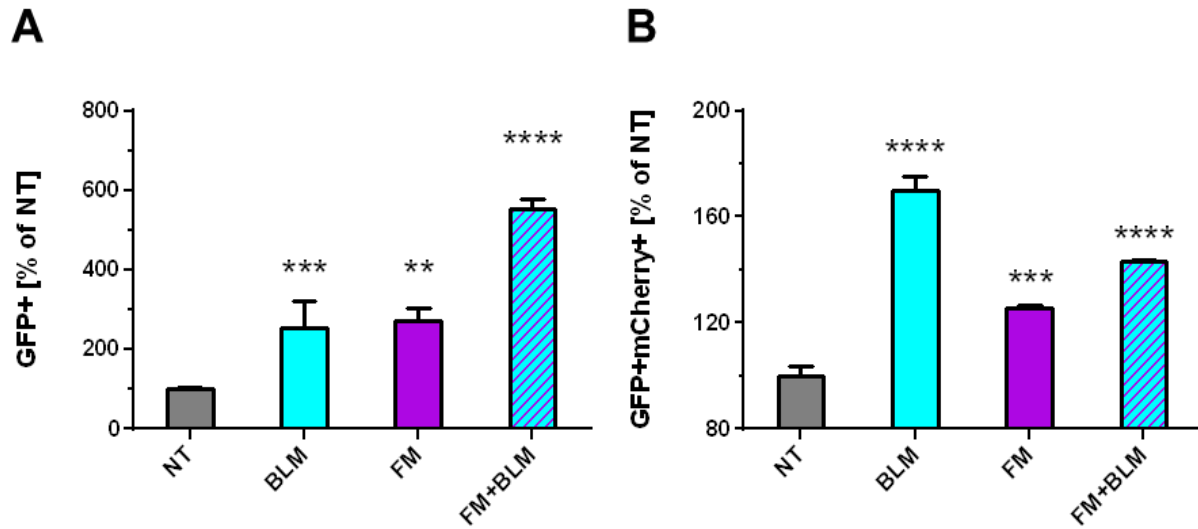
Figure 17. BLM and FANCM prevent COs independently.
Relative CO and GC frequency in U2OS CO-GC assay cells upon siRNA treatment. X-axis: different siRNA treatments; (**A**) Y-axis: percent of the cells exhibiting GFP fluorescence; values: averaged results of 1 experiment with 3 data points per treatment; error bars: standard deviation. (**B**) Y-axis: percent of the cells exhibiting GFP and mCherry fluorescence; values: averaged results of 1 experiments with 3 data points per treatment; error bars: standard deviation.

ML216 ubiquitously reduces DSBR in U2OS CO-GC cells

To examine the influence of Ml216, small particle identified as BLM inhibitor, on COs

and GCs using the CO-GC assay, I introduced the drug to the cells at the same time as adeno-I-

SceI and measured cell fluorescence three days post treatment using flow cytometry (**Fig. 18**).

The results indicate that ML216 inhibits both COs (two-fold reduction; **Fig 18A**), and GCs

(three-fold reduction; **Fig. 18B**).
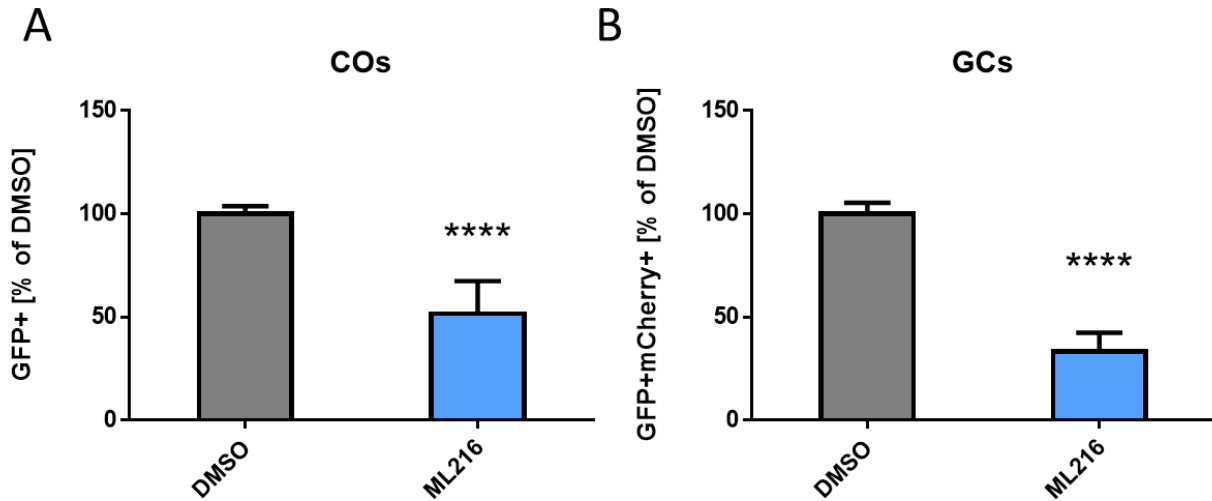
Figure 18. ML216 ubiquitously reduces COs and GCs in U2OS cells.
Relative CO and GC frequency in U2OS CO-GC assay cells upon ML216 treatment. X-axis: different drug treatments; (**A**) Y-axis: percent of the cells exhibiting GFP fluorescence; values: averaged results of 2 experiments with 6 data points per treatment; error bars: standard deviation. (**B**) Y-axis: percent of the cells exhibiting GFP and mCherry fluorescence; values: averaged results of 2 experiments with 6 data points per treatment; error bars: standard deviation.

Conclusion

The objective of the research conducted and described in this chapter is to investigate the

roles of DNA helicases in regulation of CO and GC outcomes during DSBR. First, I tested a

panel of siRNAs to assess the influence of DNA helicases on GC regulation using U2OS-

DRGFP assay (**Fig. 11**) developed by the Jasin laboratory (Pierce et al., 1999). The DR-GFP

assay is currently considered a golden standard in the field of DSBR and is widely utilized by the

scientific community. To validate the assay, and confirm the functionality of the protocol, I

depleted BRACA2 and demonstrated a three-fold decrease of GC levels as expected (**Fig. 12**).

Then, I tested siRNAs targeting BLM, FANCM, FBXO18, RECQL5, and RTEL1 (**Fig. 12**). The

results for FBXO18 and RECQL5 in U2OS were previously published (Paliwal et al., 2014),

however only FBXO18 depletion resulted in an increase of GC as previously reported; RECQL5 depletion yielded a wild-type phenotype as opposed to a decrease in GCs. BLM depletion yielded an increase in GCs that reached statistical significance using a Student T test but not ANOVA. BLM was previously reported to inhibit GCs in HEK293 cells using the same assay (Paliwal et al., 2014). Interestingly, knocking down FANCM resulted in a two-fold decrease in GC levels, while RTEL1 depletion yielded a moderate increase in GCs.

Because of the DR-GFP assay's inability to infer the origin of GCs, I designed a novel CO-GC assay, based on the GFP and mCherry fluorescence, which can determine whether a GC resulted from a CO or other type of repair. I demonstrated this assay works both in U2OS and HEK293 cells using fluorescence microscopy, and tested how the BLM and FANCM depletion influence CO/GC outcomes in this assay. BLM depletion, as predicted, leads to a three-fold increase in COs and 50% increase in GCs. The preliminary results for FANCM depletion alone and in conjunction with BLM siRNA indicate that FANCM has a similar role in CO regulation to BLM, and I observed a synergistic effect from depletion of both helicases. The synergistic effect was not present when looking at GC levels, despite how either single knockdown seem to cause GC elevation in this assay.

Lastly, I tested whether CO-GC or DR-GFP assays are compatible with a drug treatment protocol. To assess it, I used a ML216 - BLM inhibitor, causing a moderate but significant decrease in GC levels in DR-GFP assay. However, in case of the CO-GC assay, ML216 caused two and three fold decrease in CO and GC levels respectively indicating a high sensitivity of this assay. Taken together, these data indicate the novel CO-GC assay I developed is functional for analysis in human cells, compatible with siRNA, and drug treatment approaches.

Materials and Methods

Construction of assay plasmids

The crossover (CO) assay construct was based on DR-GFP and the intron-containing *mCherry* gene from pDN-D2irC6kwh (Addgene #44725). DR-GFP was cut with *Bam*HI to isolate the *iGFP* fragment and restore the original 3' *GFP* sequence. This was cloned into the *mCherry* intron. The entire *iGFP*-containing *mCherry* gene was then cloned into the DR-GFP vector cut with *Hin*dIII so that the original *iGFP* fragment was replaced.

Generation of stably transfected cell lines

U2OS and HEK293 cells were cultured under normal conditions (DMEM +10% FBS + pen/strep) for 24h till they reached 80% confluency before transfection with a CO-GC assay constructs using a Nucleofector™ 2b Device (Lonza #AAB-1001) and Cell Line Nucleofector® Kit V (Lonza #VCA-1003). One week post-transfection appropriate antibiotics were added to select for the cells with a stably-integrated construct. The SDSA assay construct contains a neo^R gene; cells receiving this construct were treated with 10 ug/ml Puromycin (Sigma # P8833) for one week and then a single-cell clones were derived.

DNA repair assay and flow cytometry

CO-GC-U2OS of DR-GFP cells were cultured in 10 cm dishes containing 10 ml of DMEM medium with high glucose; Corning) until split onto 6-well plates at a concentration of 5×10^4 cells per milliliter using 0.05% Trypsin 0.53% mM EDTA solution (Corning). Upon reaching ~60% confluency, the cell were treated with an siRNA reaction mixture (90 nmol of siRNA and 8 µl lipofectamine 2000 reagent per well; Invitrogen). 24 hours after transfection the

siRNA reaction mixture was replaced with the fresh culture medium. 12 hours later the cells were treated with 100 μl of *I-Sce*I-expressing adenovirus (Anglana and Bacchetti, 1999) (previously titrated to a non-lethal concentration); or transfected with an I-SceI-expressing vector (Jasin laboratory) using lipofectamine 2000. After another 24 hours the medium was replaced and thus the adenovirus removed. 72 hours later the cells were harvested and resuspended in 1x PBS (Corning) supplemented with 2% fetal bovine serum (FBS) and 5 mM EDTA for flow cytometry acquisition on a BD Aria sorter, using 488nm and 561nm lasers to detect the mCherry and GFP fluorescence.

Genomic DNA isolation

CO-GC U2OS cells were cultured in a 15 cm dish till they reached 100% confluency. Then they were rinsed gently with 1x PBS and harvested using 0.05% Trypsin 0.53 mM EDTA and pelleted by centrifuging for three minutes at 2000 rpm. Cells were washed with PBS and transferred to 1.5ml microfuge tubes and spun for 10 sec to re-pellet. PBS was removed and cells were resuspended in TSM + 0.5%NP-40 solution (140 mM NaCl; 10 mM Tris-HCl, pH 7.4; 1.5 mM MgCl$_2$), then incubated on ice for 2-3 minutes. After pelleting, cells were resuspended in 1 ml nuclei dropping buffer (0.075 M NaCl; 0.024 M EDTA, pH 8.0). The suspension was transferred to a 15 ml tubes containing 4 ml of nuclei dropping buffer with 1mg of Proteinase K (final Proteinase K concentration = 0.2 mg/ml), and 0.5% of SDS. The cells were lysed overnight at 37°C. The next day an equal volume of phenol was added to lysed nuclei and mixed on an orbital shaker for two hours followed by a five minute spin at 2000 rpm. The aqueous phase was transferred to a clean tube and an equal volume of chloroform was added and the mix was incubated for 30 mins on an orbital shaker. After spinning, the aqueous phase was transferred to

a new tube and 0.1 volumes of 3M sodium acetate was added, followed by one volume of isopropanol. The DNA was spooled out using a glass Pasteur pipette and resuspended overnight in 1 ml TE buffer (10 mM Tris-HCl, pH 8.0; 1 mM EDTA, pH 8.0). The next day the DNA was precipitated using 0.5 volumes of 7.5M NH_4OAc and two volumes of ethanol. DNA was spooled out and resuspended in 0.5ml TE-4 buffer (10mM Tris-HCl, pH 8.0; 0.1mM EDTA, pH 8.0). Samples were stored in 4°C until analyzed.

Statistical data analysis

GraphPad Prism 6 software (version 6.07) was utilized to generate the figures presenting the flow cytometry results of the CO-GC and DR-GFP assays. Prism also provides a statistical data analysis platform. The data was analyzed using two statistical tests; one-way ANOVA with a correction for multiple comparisons or Student T test if a single comparison was needed.

CHAPTER 4

DISCUSSION AND FUTURE DIRECTIONS

The primary objective of this dissertation is to genetically and molecularly characterize the contribution of DNA helicases to genome stability in humans. Alterations in the genetic material are a primary cause of cell lethality and cancer development, thus studying the mechanisms that ensure fidelity and efficacy during DSBR is vital. This dissertation addresses specifically DNA double-strand break repair via homologous recombination and focuses on developing novel tools necessary to study DSBR outcomes in human cells.

Overview of major findings

I was prompt to conduct the research presented in this dissertation to bridge the gap in knowledge between the DSBR studies conducted in humans and in model organisms. Since the proposal of the DSBR model by Szostak *et al* based on their work in *Saccharomycetes cerevisiae* (Szostak et al., 1983), both yeast and fruit flies have been instrumental tools in expanding our understanding of the mechanisms governing DNA repair. The canonical DSBR model predicts formation of a D-loop upon 3'-end resection, followed by DNA synthesis, and the formation and subsequent resolution of the dHJ intermediate (**Fig. 1A-E**). dHR resolution leads to a formation of COs and NCOs (**Fig1E**), however, Allers and Lichten demonstrated in yeast, that NCOs are generated much earlier than COs, indicating other NCO sources (Allers and Lichten, 2001). Since then, we learned a great deal about DNA helicases, such as Sgs1/BLM, which can either facilitate dHJ dissolution to prevent CO formation (**Fig. 1D'**)(Singh et al., 2008; Wu and

Hickson, 2003, 2006), or disrupt D-loops to prevent dHJ formation (**Fig. 1C'**) (Bachrati et al., 2006; Youds et al., 2010). Gloor and Nassif described SDSA as one of the sources of NCOs in fruit flies (Gloor et al., 1991; Nassif et al., 1994). Development of SDSA assays in *S. cerevisiae* and *Drosophila* deepened our understanding of this process and lead to a discovery of Srs2 (yeast) and BLM and FANCM helicases (fruit fly) as major SDSA regulators (Kuo et al., 2014) (Adams et al., 2003; Miura et al., 2012). Today, SDSA is thought as a predominant pathway of DSBR in mitotically dividing cells leading to NCOs and preventing recombination. Furthermore, with the recent development of CRISPR/Cas9 technology (Cong et al., 2013; Mali et al., 2013), replacement of multi-kilobase fragments after Cas9 cleavage has been suggested to occur through SDSA (Byrne et al., 2015). Paradoxically SDSA, although implied, has never been demonstrated in humans, because unlike in yeast or fruit flies, there are no assays to study SDSA in human cells.

In Chapter 2, I am presenting the design, describing the development, and highlighting the initial results from the utilization of the first human SDSA assay in U2OS (**Fig. 2**) (Ponten and Saksela, 1967) and HeLa cells (**Fig. 10**) (Scherer et al., 1953). Conceptually, the SDSA assay for human cells is similar to the $P\{w^a\}$ SDSA assay utilized in the Sekelsky laboratory (Adams et al., 2003) and consists of two non-functional *mCherry* genes. The upstream *mCherry* contains 18-bp *I-Sce*I recognition sequence replacing internal 350-bp of the original sequence; the downstream *mCherry* gene consists of two *mCherry* fragments overlapping by the 350-bp sequence, but separated by a 3-kb spacer DNA. Only SDSA, with DNA synthesis reaching at least 350-bp, leads to the restoration of the functional *mCherry* gene making the assay suitable for both, fluorescent microscopy (**Fig. 2**) and flow cytometry analysis (**Fig. 4**). Sorting and clonal expansion of the repair events has also proven to be feasible and allowed initial molecular

characterization of the events that underwent SDSA (up to 3%) or failed to do so (**Fig. 3**).

Furthermore, I validated my assays by depleting BRCA2, a protein necessary for RAD51-mediated strand invasion and homology search, and detected a pronounced decrease in SDSA

frequency as expected (**Fig. 5**). These results demonstrate convincingly that as previously

hypothesized, human cells, along with yeast and fruit fly cells, utilize SDSA to repair DSBs

(Adams et al., 2003; Miura et al., 2012). Nevertheless, SDSA levels up to 3% in human cells,

although consistent with the results derived from yeast (4.7%; Miura et al., 2012) and fruit flies

(3.8%; Adams et al., 2003), may question SDSA being a predominant pathway generating NCOs

in eukaryotic cells. One explanation for detection of such low levels of SDSA could be the

design of the assays. To visualize SDSA, all of the aforementioned assays rely on the ability of

both 3' ends to participate in the homology search and DNA invasion (**Fig. 2C**), effectively

detecting only two-ended SDSA. As depicted in the DSBR model (**Fig. 1C** and **1C'**), one-ended

SDSA is possible, and perhaps more frequent than two-ended SDSA, but challenging to detect as

yields outcomes indistinguishable from other NCOs (compare DNA synthesis tract patterns in

Fig 1C' with **Fig. 1D'** and **1E'**). Furthermore, cell cycle profiling (**Fig. 8**) indicates that less than

50% of cells reside in S-phase, when HR is promoted (Mao et al., 2008), at the time of DSB

generation and repair (see **Fig. 8C** table; Day 3). Although the human SDSA assay construct

encompasses the repair template and does not rely, unlike the $P\{w^a\}$ SDSA, on the presence of a

sister chromatid, HR (and thus SDSA) in G1 (also in G2/M) is downregulated (Mao et al., 2008),

which can contribute to lowering the numbers of mCherry positive cells.

Despite limitations, equipped with such a powerful tool such as the first SDSA assay in

human cells, I proceeded to the characterization of selected human DNA helicases. I focused on

the helicases that have been either previously reported to influence SDSA in other organisms

(BLM, FANCM), implicated in DSBR using other assays (RECQL5, FBXO18, WRN), or shown to disrupt D-loops *in vitro* (RTEL1) (**Fig. 5**). I initially hypothesized, based on the results from the SDSA assay in *Drosophila* (Adams et al., 2003), that BLM and FANCM depletion will lead to a decrease in SDSA frequency. Only the BLM and RTEL1 siRNA knockdown yielded a phenotype different than the one of the non-targeting siRNA control. Surprisingly however, it was a two-fold increase in SDSA rather than a hypothesized decrease. SDSA increase was DNA 3'end invasion and the homology search dependent, as knocking down BRCA2 in conjunction with BLM or RTEL1 resulted in a decrease of SDSA in comparison to the BLM and RTEL1 single knockdowns (**Fig. 6**). This remarkable result answered the major question concerning which helicases regulate SDSA in human cells, but lead me to attempt to address a few others; what is the mechanisms of CO prevention in mitotically dividing human cells? Is SDSA a part of it and if so, is SDSA regulated differently in human cells than in yeast and flies?

First, to gain insights into the mechanism of SDSA in human cells, I isolated 55 mCherry positive single-cell derived clones from various siRNA treatments, and utilized a PCR amplification approach with multiple primer sets (**Table 2**) to analyze them. Molecular analysis indicated that all of the events underwent SDSA leading to the restoration of *mCherry*. One event was missing the sequence intervening two *mCherry* genes indicating that SDSA was initiated, but then completed by the canonical DSBR with a dHJ intermediate. This result indicates the primary objective of the cell is to repair DNA lesions and under any circumstances allow the DSBs to prevail longer than necessary; the pathway choice comes second. The transition from SDSA to CO in this assay requires a D-loop disruption and 3'end dissociation from the proximal *mCherry* repeat with a subsequent invasion of the distal repeat, supporting the idea of a multiple

strand invasion mechanism previously indicated to be present in fruit flies (McVey et al., 2004b) and yeast (Pâques et al., 1998).

Then, I proceeded to isolate and analyze the DNA sequence from over 200 clones that did not restore the *mCherry* gene (**Fig. 7**). All of the clones derived from the non-targeting siRNA control, and most from siBLM and siRTEL1 exhibited DNA sequence patterns consistent with precise NHEJ or a lack of I-SceI cutting. The remaining clones, which were derived from the cells depleted of BLM or RTEL1 helicases, exhibited DNA sequence patterns consistent with either long-tract SDSA synthesis, dHJ resolution or dissolution, or initiated SDSA but completed using TMEJ. These finding were consisted with a proposed anti-crossover role of BLM and RTEL1 helicases (Barber et al., 2008; Chaganti et al., 1974; Wechsler et al., 2011), and indicate that human cells depleted of BLM or RTEL1 exhibit a dramatic increase in HR.

Because the anti-crossover role for BLM and other helicases is thought to be associated with their pro-SDSA role, which is supported by the findings derived from the studies in model organisms, it is perplexing how human BLM and RTEL1 can inhibit both COs and SDSA events. The molecular analysis of the repair events that failed to produce a functional *mCherry* gene in the SDSA assay revealed that the synthesis tracts were longer in the helicase depleted backgrounds. Synthesis tracts are also elongated in other DNA repair protein depleted backgrounds like BRCA1 and CtIP (Chandramouly et al., 2013). This result indicates perhaps 350-bp synthesis, required on both sides of the break, was challenging under normal conditions because of BLM and RTEL1 constantly disrupting D-loop extension. Conversely, the synthesis proceeded uninterrupted when either BLM or RTEL1 were depleted. Considering the vast majority of the DNA repair studies is conducted in either U2OS or HeLa, which are cancer cell lines established in 1967 and 1953 respectively, it is conceivable to think that their DNA repair

regulation is different than in normal human cells, or perhaps years of culturing lead to chromosome amplifications and a copy number increase of *BLM* and *RTEL1* genes. Should BLM and RTEL1 be overexpressed or hyperactive in U2OS leading to a premature D-loops disruption and SDSA inhibition, paradoxically, depleting these helicases in cancer cells could lead to the restoration of the physiological levels of SDSA presumably present in normal cells. Addressing these questions, although extremely interesting, would require developing an SDSA assay in normal cells, such as fibroblasts, and thus is beyond the scope of this work.

The levels of HR in human cells are currently assessed in the field of DNA repair using DR-GFP assay developed in the Jasin laboratory (**Fig. 11**) (Pierce et al., 1999). Although this GC assay is designed to measure all NCOs regardless of the source, some authors mistakenly attribute it also the ability to measure SDSA (Paliwal et al., 2014; Wang et al., 2011). I dedicated the first portion of Chapter 3 to the studies of GCs in different genetic backgrounds using DR-GFP assay in U2OS (**Fig. 12**). I utilized an siRNA approach to deplete BRCA2 (positive control) and five DNA helicases: BLM, FANCM, FBXO18, RECQL5, and RTEL1. Knockdown of FANCM lead to a decrease in the levels GCs, while depletion of FBXO18 or RTEL1 lead to a moderate but significant increase in GCs. GC levels were elevated in BLM deficient background but did not reach statistical significance unlike previously reported in HEK293 cells (Paliwal et al., 2014; Wang et al., 2011). These results indicate the repair event's origin detected in the DR-GFP assay is at least partially different from the one in the SDSA assay. Specifically, FANCM seems to be required for NCO formation (**Fig. 12**), but not for SDSA (**Fig. 5**). Conversely, FBXO18 appears to inhibit NCOs in DR-GFP assay (**Fig. 12**), but does not influence SDSA (**Fig. 5**). Lastly, BLM and RTEL1 have a mild effect, if any, on GCs in general with this assay (**Fig. 12**) but when depleted lead to a two-fold increase in SDSA (**Fig. 5**).

To address the role of human DNA helicases in preventing COs and regulating GCs, I designed a novel CO-GC assay for human cells (**Fig. 13**). This assay is conceptually similar to the DR-GFP assay and contains the non-functional I-SceI-interrupted *GFP* gene, however, there are major differences in its design. The repair template is a 5'end deleted *GFP* gene (5' and 3' deleted *iGFP* in DR-GFP assay) placed in an intron of a functional *mCherry* gene, but in the opposite orientation to the upstream *GFP*. The unique design of the CO-GC assay allows tracking CGs and COs using fluorescence (GFP+mCherry+ vs. GFP+ respectively) and prevents SSA occurrence. The assay is functional in U2OS (**Fig. 14**) and HEK293 cells (**Fig. 15**) as predicted, however, HEK293 cells are not compatible with the viral I-SceI delivery approach and exhibit high levels of spontaneous GCs. BLM helicase depletion in CO-GC U2OS cells leads to the elevation of CO levels which is consisted with increased SCEs observed in Bloom Syndrome patients (Chaganti et al., 1974; Wechsler et al., 2011), but also leads to the elevation of GCs which was reported before (Paliwal et al., 2014; Wang et al., 2011), and should they come from SDSA, these results would also be consistent with the increased SDSA levels observed in U2OS SDSA assay (**Fig. 5**).

Both of the assays I developed, SDSA and CO-GC, as well as the DR-GFP assay, are not only compatible with the siRNA approach, but also with various drug treatments. In this study, I used a small particle ML216, found in a screen for BLM inhibitors, as an example (Nguyen and Hickson, 2013). ML216 was documented to inhibit BLM DNA unwinding activity in *vitro* and partially recapitulate the increased SCEs phenotype characteristic to Bloom Syndrome patient cells (Nguyen and Hickson, 2013). I hypothesized, exposing U2OS-SDSA cells to ML216 will result in a phenotype similar to the one of BLM depletion using siRNA. Surprisingly, the BLM inhibitor led to a two-fold decrease in SDSA levels, rather than a two-fold increase observed in

BLM knockdown (**Fig. 9**). Further analysis using a combined siRNA and drug treatment approach revealed ML216 inhibits SDSA even in a BLM deficient background (**Fig. 9**) indicating ML216 might have other than BLM targets promoting SDSA. Another possible explanation is the levels of BLM and thus SDSA are tightly regulated in normal cells. In U2OS however, should the BLM helicase be upregulated or overexpressed, siRNA knockdown elevates SDSA levels, while ML216 addition inhibits the remaining protein and reduces SDSA. Therefore, ML216 treatment could be mimicking a BLM knockout, or making the inactivated BLM sequester other proteins required to utilize SDSA. Additionally, I tested ML216 using DR-GFP and CO-GC assays, and discovered a pronounced decrease in CO and GC levels, suggesting ML216 targets a protein responsible for the regulation of all DSBR outcomes or that inactivated BLM is poisoning HR altogether (**Fig. 12 and Fig. 18**).

Proposed model for the role of DNA helicases in DNA repair

Taken together these data strongly indicate BLM and RTEL1 helicases are major regulators of DNA DSB repair in human cells. BLM and RTEL1 prevent-long tract DNA synthesis presumably by disrupting D-loops (**Fig. 19A**). When either BLM or RTEL1 are depleted, long tract synthesis can occur which allows to synthesize 350-bp long *mCherry* fragment required to complete SDSA (**Fig. 19B**), but also facilitates a formation of long D-loops which then can be:

1) disrupted by less processive helicases, perhaps FANCM, leading to long-SDSA (**Fig. 19C**);

2) cleaved by resolvases leading to aborted SDSA, perhaps completed by TMEJ (**Fig. 19D**);

3) dHJ formation and increased CO levels as seen in CO-GC and SDSA assays (**Fig. 19E**).
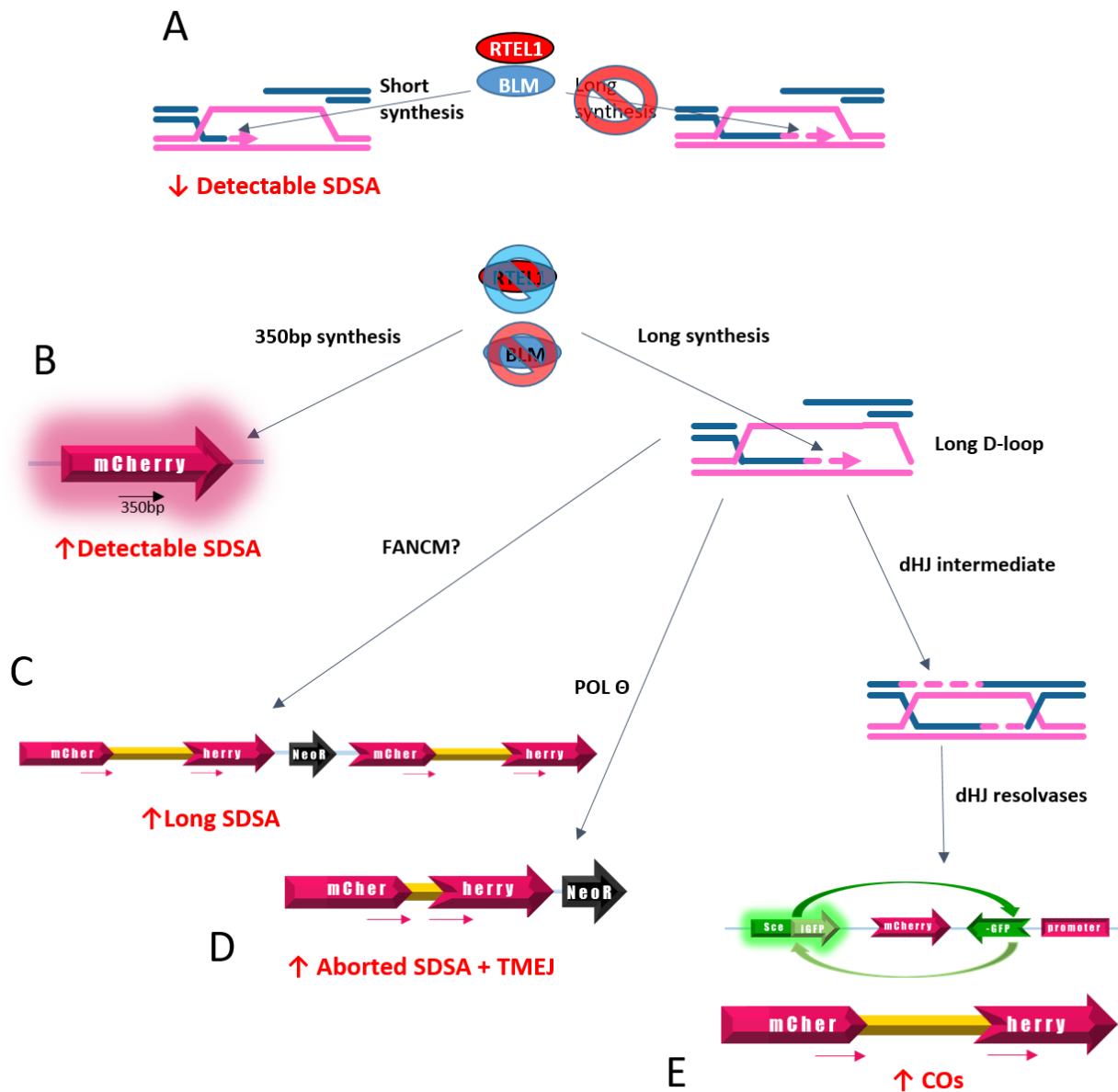
Figure 19. A model for the role of DNA helicases in DNA DSB repair.
(**A**) BLM and RTEL1 allow short-tract synthesis but prevent long-long tract synthesis by disrupting D-loops; (**B**) In BLM or RTEL1 deficient background, uninterrupted DNA synthesis of approximately 350 bp facilitates SDSA; (**C**) Long D-loops are eventually disrupted, perhaps by FANCM or another remaining helicase, which leads to the formation of long SDSA products encompassing the spacer DNA, thus rendering *mCherry* gene non-functional. (**D**) Aborted SDSA is completed my TMEJ; (**E**) Second-end capture by the long D-loop leads to a dHJ formation. This intermediate is then cleaved dHJ resolvases, which generate COs.

An alternative hypothesis could be how BLM and RTEL1 affect the cell cycle, and either

depletion leads to an elongation of S-phase where HR was shown to be preferred over NHEJ

(Mao, 2008). However, this is unlikely as I investigated the cell cycle profiles for three days after

BLM depletion and did not observe any significant increase in the number of S-phase cells

(**Fig. 8**)

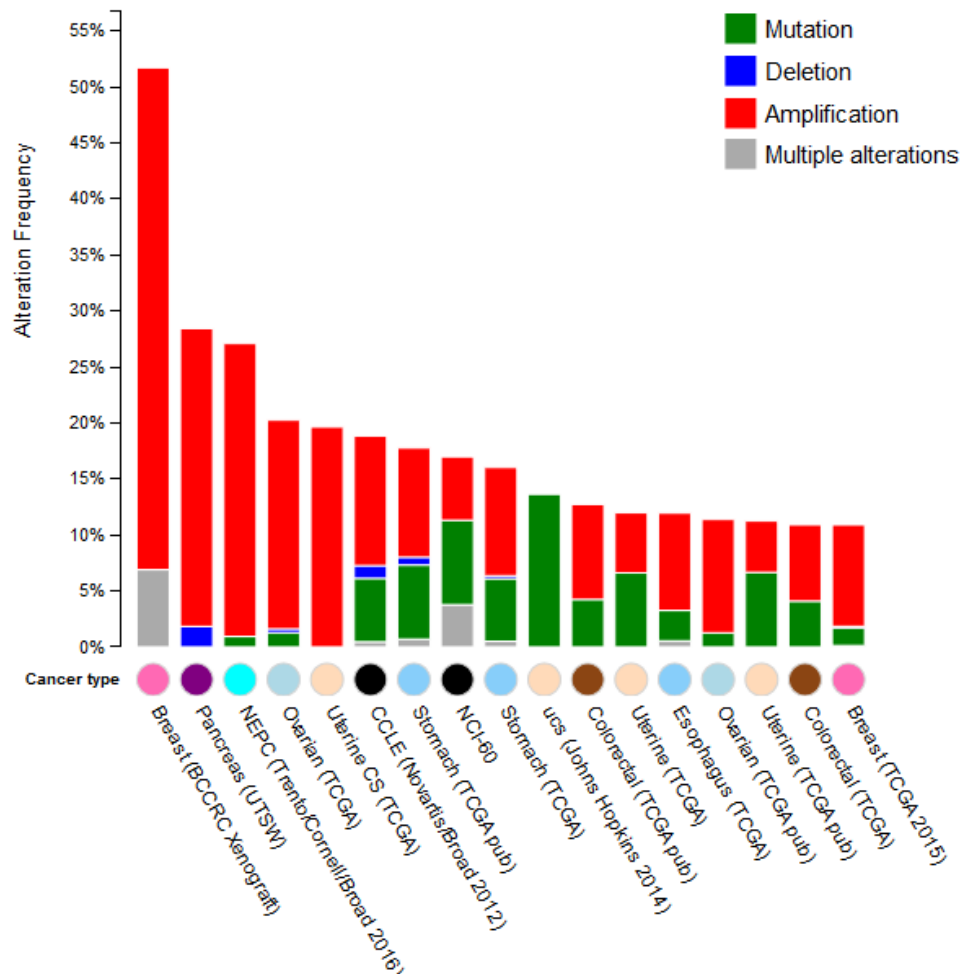**Figure 20. BLM and RTEL1 alteration frequency in various cancer types.**
A cBioPortal-generated graph representing BLM or RTEL1 alteration frequency in any given type of
cancer as indicated; Neuroendocrine Prostate Cancer (NEPC); Cancer Cell Line Encyclopedia (CCLE);
The US National Cancer Institute (NCI) 60 human tumor cell line anticancer drug screen; Uterine
Carcinosarcoma (ucs); source: www.cbioportal.org

Interestingly, a compilation of multiple cancer studies (**Fig. 20**) indicate either BLM or RTEL1 are mutated in 50% of breast cancer cases (for comparison, BRCA1 or BRCA2 are mutated in only 24%) and many other like pancreas, stomach, ovarian, and uterine cancers (20-28% of cases). Surprisingly, the vast majority of these alterations are amplifications indicating multiple copies of BLM and RTEL1 may have a negative effect on preservation of genome stability, perhaps by premature D-loop disruption and a complete suppression of SDSA, which would be consistent with the increase levels of SDSA upon helicase depletion.

Future Directions

The objective of this dissertation was to assess the role of DNA helicases in genome stability, especially in the contest of SDSA, GC and CO regulation. While, the work I conducted addresses the main question of which preselected helicases contribute to the aforementioned DNA repair outcomes and hints on the possible mechanism, there are other fascinating questions deriving from this research.

Testing DNA helicases which are thought to disrupt D-loops or have been found to influence SDSA in other organisms was only the beginning. There are other candidate helicases to analyze their contribution to DSB repair outcomes using SDSA and CO-GC assays. Recently, MCM8 and MCM9 have been found to influence gametogenesis and homologous recombination in mice (Lutzmann et al., 2012), as well as to promote DNA resection of the MRN complex (Mre11- Rad50-NBS1) and thus influence the choice between NHEJ and HR (Lee et al., 2015). Irc20 is a poorly characterized putative DNA helicase that came out from the yeast studies, next to Srs2, as a positive SDSA regulator (Miura et al., 2012); finding and testing Irc20 human ortholog could benefit our understanding of SDSA regulation in human cells.

Molecular analysis of the BLM and RTEL1 deficient cells using the SDSA assay revealed that the repair events exhibit long-tract synthesis (**Fig. 7**). Long-tract synthesis has been observed to occur in BRCA1 and CtIP deficient cells using a GC assay developed by the Scully laboratory (Chandramouly et al., 2013) making these two proteins good candidates for SDSA regulation. Furthermore, CtIP-BRCA1 complex modulates the choice of DSB repair pathway throughout the cell cycle and CtIP-BRCA1 interaction is necessary not only to promote HR during S-phase but also to promote microhomology-mediated end-joining (MMEJ) in G1 (Yun and Hiom, 2009).

Ten single-cell derived clones of the SDSA assay repair events, that occurred in BLM or RTEL1 depleted cells, exhibited a repair pattern consistent with initiated SDSA but completed by another form of end-joining, called theta-mediated end-joining (TMEJ). Polymerase theta, which has been found essential for TMEJ (Wyatt et al., 2016), contains a putative helicase domain. Its role outside TMEJ is purely speculative but could be tested using SDSA and CO-GC assays.

While the Sekelsky laboratory utilizes the Drosophila SDSA assay to study helicases, McVey laboratory focuses on translesion synthesis (TLS) polymerases, which a number of was shown to be necessary for SDSA in fruit flies (Kane et al., 2012). Polymerases zeta and REV1 were shown to promote GCs in DR-GFP HeLa cells (Sharma and Canman, 2012), yet their role in SDSA remains to be elucidated. McVey *et al* also showed there are multiple cycles of strand invasion during double-strand gap repair in Drosophila (McVey et al., 2004b). Although the SDSA assay in its current design cannot adequately assess whether it also be true for human cells, after introducing a number of single nucleotide polymorphisms (SNPs) to the repair template *mCherry* gene this assessment would be feasible.

The search for genes regulating the SDSA or CO/GC outcomes is not limited to DNA helicases or TLS polymerases. UNC offers services of the RNAi HTS Facility that manages a human genomic siRNA library from Dharmacon, composed of ~84,500 siRNAs targeting 21,125 genes (Ref Seq database v5.0-8.0), which presents a compelling alternative to the aforementioned candidate gene approaches.

With the recent development of CRISPR/Cas9 technology of genome editing (Cong et al., 2013; Mali et al., 2013), one idea would be to introduce DSBs at the *I-Sce*I recognition sequence using Cas9 instead of I-SceI. I-SceI cleavage leaves 4 nt 3' overhangs while Cas9 generates blunt ends. Both types of DSBs could be processed differently and thus lead to different repair outcomes. The pathway choice analysis, using both SDSA and CO-GC assays, would be of great importance in light of recent studies suggesting the replacement of multi-kilobase fragments after Cas9 cleavage occurs through SDSA (Byrne et al., 2015). Additionally, Cas9 can be utilized to deliver DSBs at various locations of the repair assay constructs, which would allow assessing the minimal homologous sequence length necessary to support BRCA2-RAD51-mediated strand invasion and homology search.

Finally, the CRISPR/Cas9 system can be utilized to knockout or knock-in a helicase of interest. The major criticism of utilizing siRNA approaches to study gene functions is the inability to observe the phenotype exhibited by the cells devoid of studied protein. The CRISPR/Cas9 approach can bypass this issue, however it works best in the cell lines which, unlike U2OS or HeLa, are strictly haploid or diploid, and thus possess a mere one or two copies of the to-be-removed gene. Considering the majority of DNA helicase genes, BLM and RTEL1 being a perfect example, is amplified in cancer cells (**Fig. 20**), helicase overexpression or

CRISPR/Cas9 knock-in can lead to further understanding of SDSA, GC, and CO regulation in cancer, and ultimately to a helicase-targeted drug treatment therapy.

SDSA and CO-GC assays are fully compatible with drug treatment approaches as demonstrated in this dissertation using ML216 as an example (**Fig. 9 and Fig. 18**). In fact, the BLM inhibitor results proved to be most intriguing, as the dramatically decreased SDSA phenotype prevails even when BLM helicase is depleted. Because ML216 is a DNA mimetic (Nguyen et al 2013), it is conceivable to hypothesize other than BLM targets in the cell. Finding these targets could be the key to understanding DSB repair regulation in human cells.

Conclusion

In conclusion, understanding the roles of the players involved in genome stability in humans, DNA helicases included, is of great interest for scientific community given the most recent Nobel prize was awarded for advancements in the field of DNA double-strand break repair in human cells. The original work presented in this dissertation concerning human DNA helicases is a small but significant contribution to this field. The tools developed while conducting this work, namely SDSA and CO-GC assays, offer a virtually limitless potential for improving our comprehension of the mechanisms that guard human genome.

REFERENCES

Adams, M.D., McVey, M., and Sekelsky, J. (2003). *Drosophila* BLM in double-strand break repair by synthesis-dependent strand annealing. Science *299*, 265-267.

Allers, T., and Lichten, M. (2001). Differential timing and control of noncrossover and crossover recombination during meiosis. Cell *106*, 47-57.

Andersen, S.L., Kuo, H.K., Savukoski, D., Brodsky, M.H., and Sekelsky, J. (2011). Three structure-selective endonucleases are essential in the absence of BLM helicase in *Drosophila*. PLoS Genet *7*, e1002315.

Andersen, S.L., and Sekelsky, J. (2010). Meiotic versus mitotic recombination: two different routes for double-strand break repair: the different functions of meiotic versus mitotic DSB repair are reflected in different pathway usage and different outcomes. Bioessays *32*, 1058-1066.

Anglana, M., and Bacchetti, S. (1999). Construction of a recombinant adenovirus for efficient delivery of the *I-Sce*I yeast endonuclease to human cells and its application in the in vivo cleavage of chromosomes to expose new potential telomeres. Nucleic Acids Res *27*, 4276-4281.

Bachrati, C.Z., Borts, R.H., and Hickson, I.D. (2006). Mobile D-loops are a preferred substrate for the Bloom's syndrome helicase. Nucleic Acids Res *34*, 2269-2279.

Barber, L.J., Youds, J.L., Ward, J.D., McIlwraith, M.J., O'Neil, N.J., Petalcorin, M.I., Martin, J.S., Collis, S.J., Cantor, S.B., Auclair, M.*, et al.* (2008). RTEL1 maintains genomic stability by suppressing homologous recombination. Cell *135*, 261-271.

Bignon, Y. (2004). Biological basis of cancer predisposition pp 11-20 in Genetics Predisposotion to Cancer Genetic Predisposition to Cancer *2Ed*, 11-20.

Byrne, S.M., Ortiz, L., Mali, P., Aach, J., and Church, G.M. (2015). Multi-kilobase homozygous targeted gene replacement in human induced pluripotent stem cells. Nucleic Acids Res *43*, e21.

Chaganti, R.S., Schonberg, S., and German, J. (1974). A manyfold increase in sister chromatid exchanges in Bloom's syndrome lymphocytes. Proc Natl Acad Sci USA *71*, 4508-4512.

Chandramouly, G., Kwok, A., Huang, B., Willis, N.A., Xie, A., and Scully, R. (2013). BRCA1 and CtIP suppress long-tract gene conversion between sister chromatids. Nat Commun *4*, 2404.

Chiolo, I., Minoda, A., Colmenares, S.U., Polyzos, A., Costes, S.V., and Karpen, G.H. (2011). Double-strand breaks in heterochromatin move outside of a dynamic HP1a domain to complete recombinational repair. Cell *144*, 732-744.

Chiolo, I., Saponaro, M., Baryshnikova, A., Kim, J.H., Seo, Y.S., and Liberi, G. (2007). The human F-Box DNA helicase FBH1 faces *Saccharomyces cerevisiae* Srs2 and postreplication repair pathway roles. Mol Cell Biol *27*, 7439-7450.

Chu, W. (2015). FBH1 influences DNA replication fork stability and homologous recombination through ubiqitylation of RAD51. Nat Commun *6:5931*, 1-9.

Cong, L., Ran, F.A., Cox, D., Lin, S., Barretto, R., Habib, N., Hsu, P.D., Wu, X., Jiang, W., Marraffini, L.A., *et al.* (2013). Multiplex genome engineering using CRISPR/Cas systems. Science *339*, 819-823.

Creighton, H.B., and McClintock, B. (1931). A correlation of cytological and genetical crossing-over in *Zea mays*. Proc Natl Acad Sci USA *17*, 492-497.

Crismani, W., Girard, C., Froger, N., Pradillo, M., Santos, J.L., Chelysheva, L., Copenhaver, G.P., Horlow, C., and Mercier, R. (2012). FANCM limits meiotic crossovers. Science *336*, 1588-1590.

D'Andrea, A., and Grompe, M. (2003). The Fanconi anaemia/BRCA pathway. Nat Rev Cancer *3*, 23-34.

De Muyt, A., Jessop, L., Kolar, E., Sourirajan, A., Chen, J., Dayani, Y., and Lichten, M. (2012). BLM helicase ortholog Sgs1 is a central regulator of meiotic recombination intermediate metabolism. Mol Cell *46*, 43-53.

Dervins, R. (2006). Mrc1 and Srs2 are major actors in the regulation of spontaneous crossover. EMBO J *25*, 2837– 2846.

Ding, H. (2004). Regulation of Murine Telomere Length by Rtel: An Essential Gene Encoding a Helicase-like Protein. Cell *17*, 873-886.

Ellis, N.A., Groden, J., Ye, T.Z., Straughen, J., Lennon, D.J., Ciocci, S., Proytcheva, M., and German, J. (1995). The Bloom's syndrome gene product is homologous to RecQ helicases. Cell *83*, 655-666.

Fairman-Williams (2010). SF1 and SF2 helicases: family matters. Current opinion in structural biology *20*, 313-324.

Gangloff, S., McDonald, J.P., Bendixen, C., Arthur, L., and Rothstein, R. (1994). The yeast type I topoisomerase Top3 interacts with Sgs1, a DNA helicase homolog: a potential eukaryotic reverse gyrase. Mol Cell Biol *14*, 8391-8398.

Gloor, G.B., Nassif, N.A., Johnson-Schlitz, D.M., Preston, C.R., and Engels, W.R. (1991). Targeted gene replacement in *Drosophila* via *P* element- induced gap repair. Science *253*, 1110-1117.

Holliday, R. (1964). A mechanism for gene conversion in fungi. Genetical research *78*, 282-304.

Hu, Y., Lu, X., Barnes, E., Yan, M., Lou, H., and Luo, G. (2005). Recql5 and Blm RecQ DNA helicases have nonredundant roles in suppressing crossovers. Mol Cell Biol *25*, 3431-3442.

Huang, M., Kim, J.M., Shiotani, B., Yang, K., Zou, L., and D'Andrea, A.D. (2010). The FANCM/FAAP24 complex is required for the DNA interstrand crosslink-induced checkpoint response. Mol Cell *39*, 259-268.

Ira, G., Malkova, A., Liberi, G., Foiani, M., and Haber, J.E. (2003). Srs2 and Sgs1-Top3 suppress crossovers during double-strand break repair in yeast. Cell *115*, 401-411.

Kane, D.P., Shusterman, M., Rong, Y., and McVey, M. (2012). Competition between replicative and translesion polymerases during homologous recombination repair in *Drosophila*. PLoS Genet *8*, e1002659.

Kim, J. (2004). SCFhFBH1 can act as helicase and E3 ubiquitin ligase. Nucleic Acids Res *32*, 2287–2297.

Kitato, S. (1999). Mutations in RECQL4 cause a subset of cases of Rothmund-Thomson syndrome. Nat Genet *22*, 82–84.

Knudson, A.G., Jr. (1971). Mutation and cancer: statistical study of retinoblastoma. Proc Natl Acad Sci USA *68*, 820-823.

Krejci, L. (2003). DNA helicase Srs2 disrupts the Rad51 presynaptic filament. Nature *423*, 305–309.

Kuo, H.K., McMahan, S., Rota, C.M., Kohl, K.P., and Sekelsky, J. (2014). *Drosophila* FANCM helicase prevents spontaneous mitotic crossovers generated by the MUS81 and SLX1 nucleases. Genetics *198*, 935-945.

Kurkulos, M., Weinberg, J.M., Roy, D., and Mount, S.M. (1994). *P* element-mediated *in vivo* deletion analysis of *white-apricot*: deletions between direct repeats are strongly favored. Genetics *136*, 1001-1011.

LaRocque, J.R., Stark, J.M., Oh, J., Bojilova, E., Yusa, K., Horie, K., Takeda, J., and Jasin, M. (2011). Interhomolog recombination and loss of heterozygosity in wild-type and Bloom syndrome helicase (BLM)-deficient mammalian cells. Proc Natl Acad Sci USA *108*, 11971-11976.

Lee, K., Im, J., Shibata, E., Park, J., Handa N, SC, K., and A, D. (2015). MCM8-9 complex promotes resection of double-strand break ends by MRE11-RAD50-NBS1 complex. nature communications *6*.

Liu, P., Lacaria, M., Zhang, F., Withers, M., Hastings, P.J., and Lupski, James R. (2011). Frequency of Nonallelic Homologous Recombination Is Correlated with Length of Homology: Evidence that Ectopic Synapsis Precedes Ectopic Crossing-Over. The American Journal of Human Genetics *89*, 580-588.

Lorenz, A., Osman, F., Sun, W., Nandi, S., Steinacher, R., and Whitby, M.C. (2012). The fission yeast FANCM ortholog directs non-crossover recombination during meiosis. Science *336*, 1585-1588.

Luo, G., Santoro, I.M., McDaniel, L.D., Nishijima, I., Mills, M., Youssoufian, H., Vogel, H., Schultz, R.A., and Bradley, A. (2000). Cancer predisposition caused by elevated mitotic recombination in Bloom mice. Nat Genet *26*, 424-429.

Lutzmann, M., Grey, C., Traver, S., Ganier, O., Maya-Mendoza, A., Ranisavljevic, N., Bernex, F., Nishiyama, A., Montel, N., Gavois, E.*, et al.* (2012). MCM8- and MCM9-deficient mice reveal gametogenesis defects and genome instability due to impaired homologous recombination. Mol Cell *47*, 523-534.

Mali, P., Yang, L., Esvelt, K.M., Aach, J., Guell, M., DiCarlo, J.E., Norville, J.E., and Church, G.M. (2013). RNA-guided human genome engineering via Cas9. Science *339*, 823-826.

Mao, Z. (2008). DNA repair by nonhomologous end joining and homologous recombination during cell cycle in human cells. cell cycle *7*, 2902-2906.

McVey, M., Adams, M.D., Staeva-Vieira, E., and Sekelsky, J.J. (2004a). Evidence for multiple cycles of strand invasion during repair of double-strand gaps in Drosophila. Genetics *167*, 699-705.

McVey, M., Larocque, J.R., Adams, M.D., and Sekelsky, J.J. (2004b). Formation of deletions during double-strand break repair in *Drosophila* DmBlm mutants occurs after strand invasion. Proc Natl Acad Sci USA *101*, 15694-15699.

Meetei, A.R., Medhurst, A.L., Ling, C., Xue, Y., Singh, T.R., Bier, P., Steltenpool, J., Stone, S., Dokal, I., Mathew, C.G.*, et al.* (2005). A human ortholog of archaeal DNA repair protein Hef is defective in Fanconi anemia complementation group M. Nat Genet *37*, 958-963.

Merker, J.D., Dominska, M., and Petes, T.D. (2003). Patterns of heteroduplex formation associated with the initiation of meiotic recombination in the yeast *Saccharomyces cerevisiae*. Genetics *165*, 47-63.

Mitchel, K., Lehner, K., and Jinks-Robertson, S. (2013). Heteroduplex DNA position defines the roles of the Sgs1, Srs2, and Mph1 helicases in promoting distinct recombination outcomes. PLoS Genet *9*, e1003340.

Miura, T. (2013). Putative antirecombinase Srs2 DNA helicase promotes noncrossover homologous recombination avoiding loss of heterozygosity. Proc Natl Acad Sci USA *110*, 16067–16072.

Miura, T., Yamana, Y., Usui, T., Ogawa, H.I., Yamamoto, M.T., and Kusano, K. (2012). Homologous recombination via synthesis-dependent strand annealing in yeast requires the Irc20 and Srs2 DNA helicases. Genetics *191*, 65-78.

Moldovan, G.L. (2009). How the fanconi anemia pathway guards the genome. Annu Rev Genet *43*, 223–249.

Morgan, T.H., Sturtevant, A.H., Muller, H.J., and Bridges, C.B. (1915). The Mechanism of Mendelian Heredity New York: Henry Holt.

Nassif, N., Penney, J., Pal, S., Engels, W.R., and Gloor, G.B. (1994). Efficient copying of nonhomologous sequences from ectopic sites via P-element-induced gap repair. Mol Cell Biol *14*, 1613-1625.

Nguyen, G., and Hickson, I.D. (2013). a small molecule inhibitor of the BLM helicase modulates chromosome stability in human cells. chem biol *20*, 55-62.

Nimonkar, A.V., Özsoy, A.Z., Genschel, J., Modrich, P., and Kowalczykowski, S.C. (2008). Human exonuclease 1 and BLM helicase interact to resect DNA and initiate DNA repair. Proc Natl Acad Sci USA *105*, 16906-16911.

Paliwal, S., Kanagaraj, R., Sturzenegger, A., Burdova, K., and Janscak, P. (2014). Human RECQ5 helicase promotes repair of DNA double-strand breaks by synthesis-dependent strand annealing. Nucleic Acids Res *42*, 2380-2390.

Pâques, F., Leung, W.Y., and Haber, J.E. (1998). Expansions and contractions in a tandem repeat induced by double-strand break repair. Mol Cell Biol *18*, 2045-2054.

Pierce, A.J., Johnson, R.D., Thompson, L.H., and Jasin, M. (1999). XRCC3 promotes homology-directed repair of DNA damage in mammalian cells. Genes Dev *13*, 2633-2638.

Ponten, J., and Saksela, E. (1967). Two established in vitro cell lines from human mesenchymal tumours. Int J Cancer *15*, 434-437.

Resnick, M.A. (1976). The repair of double-strand breaks in DNA; a model involving recombination. J theor BioL *59*, 97-106.

Romero, N.-E., Matson, S.W., and Sekelsky, J. (2016). Biochemical activities and genetic functions of the *Drosophila melanogaster* FANCM helicase in DNA repair. Genetics *204*, 531-541.

Rong, L. (1991). The hyper-gene conversion hpr5-1 mutation of Saccharomyces cerevisiae is an allele of the SRS2/RADH gene. Genetics *127*.

Rong, L., and Klein, H. (1993). Purification and characterization of the SRS2 DNA helicase of the yeast Saccharomyces cerevisiae. J Biol Chem *268*, 1252–1259.

Ryu, T., Spatola, B., Delabaere, L., Bowlin, K., Hopp, H., Kunitake, R., Karpen, G.H., and Chiolo, I. (2015). Heterochromatic breaks move to the nuclear periphery to continue recombinational repair. Nat Cell Biol *17*, 1401-1411.

Sarek, G., Vannier, J.B., Panier, S., Petrini, J.H., and Boulton, S.J. (2015). TRF2 recruits RTEL1 to telomeres in S phase to promote T-Loop unwinding. Mol Cell *57*, 622-635.

Savage, S., and Alter, B. (2009). Dyskeratosis Congenita. Hematol Oncol Clin North Am *23*, 215-231.

Scherer, W.F., Syverton, J.T., and Gey, G.O. (1953). Studies on the propagation in vitro of poliomyelitis viruses. IV. Viral multiplication in a stable strain of human malignant epithelial cells (strain HeLa) derived from an epidermoid carcinoma of the cervix. J exp med *97*, 695-710.

Seguela-Arnaud, M., Crismani, W., Larcheveque, C., Mazel, J., Froger, N., Choinard, S., Lemhemdi, A., Macaisne, N., Van Leene, J., Gevaert, K.*, et al.* (2015). Multiple mechanisms limit meiotic crossovers: TOP3alpha and two BLM homologs antagonize crossovers in parallel to FANCM. Proc Natl Acad Sci USA *112*, 4713-4718.

Sharan, S.K., Morimatsu, M., Albrecht, U., Lim, D.S., Regel, E., Dinh, C., Sands, A., Eichele, G., Hasty, P., and Bradley, A. (1997). Embryonic lethality and radiation hypersensitivity mediated by Rad51 in mice lacking Brca2. Nature *386*, 804-810.

Sharma, S., and Canman, C. (2012). REV1 and DNA polymerase zeta in DNA interstrand crosslink repair. environ Mol Mutagen *53*, 725-740.

Singh, T.R., Ali, A.M., Busygina, V., Raynard, S., Fan, Q., Du, C.H., Andreassen, P.R., Sung, P., and Meetei, A.R. (2008). BLAP18/RMI2, a novel OB-fold-containing protein, is an essential component of the Bloom helicase-double Holliday junction dissolvasome. Genes Dev *22*, 2856-2868.

Suhasini, A.N., and Brosh, R.M., Jr. (2012). Fanconi anemia and Bloom's syndrome crosstalk through FANCJ-BLM helicase interaction. Trends Genet *28*, 7-13.

Sun, W., Nandi, S., Osman, F., Ahn, J.S., Jakovleska, J., Lorenz, A., and Whitby, M.C. (2008). The FANCM ortholog Fml1 promotes recombination at stalled replication forks and limits crossing over during DNA double-strand break repair. Mol Cell *32*, 118-128.

Symington, L.S. (2002). Role of RAD52 epistasis group genes in homologous recombination and double-strand break repair. Microbiol Mol Biol Rev *66*, 630-670.

Szostak, J.W., Orr-Weaver, T.L., Rothstein, R.J., and Stahl, F.W. (1983). The double-strand-break repair model for recombination. Cell *33*, 25-35.

van Brabant, A.J., Stan, R., and Ellis, N. (2000). DNA helicases, genomic instability, and human genetic disease. Annu Rev Genomics Hum Genet *1*, 409-459.

Vannier, J.B. (2013). RTEL1 is a replisome-associated helicase that promotes telomere and genome-wide replication. Science *342*, 239–242.

Vannier, J.B., and Sarek, G. (2014). RTEL1: functions of a disease-associated helicase. Trends Cell Biol *24*, 416–425.

Veaute, X. (2005). UvrD helicase, unlike Rep helicase, dismantles RecA nucleoprotein filaments in Escherichia coli. EMBO J *24*, 180–189.

Veaute, X., Jeusset, J., Soustelle, C., Kowalczykowski, S.C., Le Cam, E., and Fabre, F. (2003). The Srs2 helicase prevents recombination by disrupting Rad51 nucleoprotein filaments. Nature *423*, 309-312.

Vinciguerra, P., and D'Andrea, A.D. (2009). FANCM: A landing pad for the Fanconi Anemia and Bloom's Syndrome complexes. Mol Cell *36*, 916-917.

Wang, A.D. (2007). Emergence of a DNA-damage response network consisting of Fanconi anaemia and BRCA. Nat Rev Genet *8*, 735–748.

Wang, Y., Smith, K., Waldman, B.C., and Waldman, A.S. (2011). Depletion of the bloom syndrome helicase stimulates homology-dependent repair at double-strand breaks in human chromosomes. DNA Repair (Amst) *10*, 416-426.

Watson, J.D., and Crick, F.H.C. (1953). Molecular structure of nucleic acids. Nature *171*, 737-738.

Watt, P.M., Hickson, I.D., Borts, R.H., and Louis, E.J. (1996). *SGS1*, a homologue of the Bloom's and Werner's syndrome genes, is required for maintenance of genome stability in *Saccharomyces cerevisiae*. Genetics *144*, 935-945.

Watt, P.M., Louis, E.J., Borts, R.H., and Hickson, I.D. (1995). Sgs1: a eukaryotic homolog of E. coli RecQ that interacts with topoisomerase II in vivo and is required for faithful chromosome segregation. Cell *81*, 253-260.

Wechsler, T., Newman, S., and West, S.C. (2011). Aberrant chromosome morphology in human cells defective for Holliday junction resolution. Nature *471*, 642-646.

Wu, L., and Hickson, I.D. (2003). The Bloom's syndrome helicase suppresses crossing over during homologous recombination. Nature *426*, 870-874.

Wu, L., and Hickson, I.D. (2006). DNA helicases required for homologous recombination and repair of damaged replication forks. Annu Rev Genet *40*, 279-306.

Wyatt, D.W., Feng, W., Conlin, M.P., Yousefzadeh, M.J., Roberts, S.A., Mieczkowski, P., Wood, R.D., Gupta, G.P., and Ramsden, D.A. (2016). Essential roles for polymerase theta-mediated end joining in the repair of chromosome breaks. Mol Cell *63*, 662-673.

Xu, K., Wu, X., Tompkins, J.D., and Her, C. (2012). Assessment of anti-recombination and double-strand break-induced gene conversion in human cells by a chromosomal reporter. J Biol Chem *287*, 29543-29553.

Youds, J.L., Mets, D.G., McIlwraith, M.J., Martin, J.S., Ward, J.D., NJ, O.N., Rose, A.M., West, S.C., Meyer, B.J., and Boulton, S.J. (2010). RTEL-1 enforces meiotic crossover interference and homeostasis. Science *327*, 1254-1258.

Yu, C.-E., Oshima, J., Fu, Y.-H., Wijsman, E.M., Hisama, F., Alisch, R., Metthews, S., Nakura, J., Miki, T., Ouais, S.*, et al.* (1996). Positional cloning of the Werner's syndrome gene. Science *272*, 258-262.

Yun, M., and Hiom, K. (2009). CtIP-BRCA1 modulates the choice of DNA double-strand-break repair pathway throughout the cell cycle. Nature *458*, 460-463.

Zhu, Z., Chung, W.H., Shim, E.Y., Lee, S.E., and Ira, G. (2008). Sgs1 helicase and two nucleases Dna2 and Exo1 resect DNA double-strand break ends. Cell *134*, 981-994.